Hamde M. Y. Hamed

AN EXPERIMENTAL INVESTIGATION OF OPTIMUM DESIGN NEW CONFIGURATION OF THE SAVONIUS ROTOR THROUGH OPEN WIND TUNNEL EXPERIMENTS AT LOW WIND SPEED CONDITIONS

NEU 2017

AN EXPERIMENTAL INVESTIGATION OF OPTIMUM DESIGN NEW CONFIGURATION OF THE SAVONIUS ROTOR THROUGH OPEN WIND TUNNEL EXPERIMENTS AT LOW WIND SPEED CONDITIONS

A THESIS SUBMITTED TO THE GRADUATE SCHOOL OF APPLIED SCIENCES

OF

NEAR EAST UNIVERSITY

By

Hamde M. Y. Hamed

In Partial Fulfillment of the Requirements for the Degree of Master of Science in Mechanical Engineering

NICOSIA, 2017

AN EXPERIMENTAL INVESTIGATION OF OPTIMUM DESIGN NEW CONFIGURATION OF THE SAVONIUS ROTOR THROUGH OPEN WIND TUNNEL EXPERIMENTS AT LOW WIND SPEED CONDITIONS

A THESIS SUBMITTED TO THE GRADUATE SCHOOL OF APPLIED SCIENCES

OF

NEAR EAST UNIVERSITY

By

Hamde M. Y. Hamed

In Partial Fulfillment of the Requirements for the Degree of Master of Science in Mechanical Engineering

NICOSIA, 2017

Hamde HAMED: AN EXPERIMENTAL INVESTIGATION OF OPTIMUM DESIGN NEW CONFIGURATION OF THE SAVONIUS ROTOR THROUGH OPEN WIND TUNNEL EXPERIMENTS AT LOW WIND SPEED CONDITIONS

Approval of Director of Graduate School of

Applied Sciences

Prof. Dr. Nadire ÇAVUŞ

We certify this thesis is satisfactory for the award of the degree of master of science in Mechanical Engineering

Examining Committee in Charge:

I hereby declare that, all the information in this document has been obtained and presented in accordance with academic rules and ethical conduct. I also declare that, as required by these rules and conduct, I have fully cited and referenced all material and results that are not original to this work.

Name, Last Name :

Signature :

Date:

ACKNOWLEDGEMENTS

First and foremost, I would like to thank my supervisor, Assist. Prof. Dr. Hüseyin ÇAMUR, for his helpful expertise, encouragements, and advice during the research period. His amiable disposition, penetrating critiques and consistent mentoring have made my study and stay in Sheffield memorable, indeed I am very grateful.

Furthermore, I would like to thank Dr. Youssef Kassem for the many fruitful discussions that contributed to the success of this study. I always feel lucky to be with so many excellent researchers. Thanks are due to all colleagues of my institute, who were always quite helpful during my stay.

Finally, to my parents, brothers and sisters, I say thank you for all your supports through prayers and advice of encouragements to hold on, especially when my morale was low.

Thank you for all unconditional support with my studies

ABSTRACT

This study introduces a new configuration of the Savonius wind turbine to improve the performance of the conventional Savonius wind turbine. The objective of the research is to study experimentally the effect of blade geometries on the aerodynamics of unconventional Savonius wind rotors. Therefore, the rotors were tested in the subsonic open wind tunnel. In order to clarify the effect of blade geometries, static torque and mechanical power were estimated with various blade heights, blade thickness and overlap ratio at a range of 3 m/s to 13 m/s. The results indicate that all the unconventional Savonius rotors have positive static torque at all the rotor angles. Moreover, unconventional Savonius rotors at an overlap ratio of 0.0, the blade height of 700mm and blade thickness of 3 mm have a higher mechanical power compared to rotors. Furthermore, the results show also that the mechanical power increases by reducing the overlap ratio.

Keyword: Savonius; static torque; mechanical power; aspect ratio; blade thickness; overlap ratio

ÖZET

Bu çalışma, geleneksel Savonius rüzgar türbininin performansını artırmak için Savonius rüzgar türbininin yeni bir yapılandırmasını ortaya koymaktadır. Araştırmanın amacı, bıçak geometrilerinin geleneksel olmayan Savonius rüzgar rotorlarının aerodinamiği üzerindeki etkisini deneysel olarak incelemektir. Bu nedenle, rotorlar, sesaltı açık rüzgar tünelinde test edilmiştir. Bıçak geometrilerinin etkisini netleştirmek için, statik tork ve mekanik güç, çeşitli bıçak yükseklikleri, bıçak kalınlığı ve örtüşme oranı ile 3 m/s ile 13 m/s arasında değiştiği tahmin edildi. Sonuçlar, tüm alışılmamış geleneksel olmayan Savonius rotorlarının, tüm rotor açılarında pozitif statik torka sahip olduğunu göstermektedir. Buna ek olarak, 0.0 örtüşme oranı, 2.2 en-boy oranı ve 3 mm bıçak kalınlığı olan alışılmamış geleneksel olmayan Savonius rotorları diğer rotorlara kıyasla daha yüksek bir mekanik güce sahiptir. Dahası sonuçlar, mekanik gücün örtüşme oranını azaltarak arttığını da göstermektedir.

Anahtar Kelimeler: Savonius; Statistik tork; Mekanik güç; En / boy oranı; Bıçak Örtüşme oranı

TABLE OF CONTENTS

ACKNOWLEDGEMENT ii
ABSTRACT iv
ÖZET v
TABLE OF CONTENTS vi
LIST OF TABLES viii
LIST OF FIGURES ix
LIST OF SYMBOLS xiii

CHAPTER 1: INTRODUCTION 1
1.1 Background of the Study 1
1.2 Research Goals 1
1.3 Research Outline 2

CHAPTER 2: WIND TURBINE BACKGROUND 3
2.1 Wind Introduction 3
2.1.1 Power Density 3
2.1.2 Wind Speed 4
2.1.3 Power Coefficient 5
2.1.4 Tip Speed Ratio 5
2.2 Wind Turbine Classification 5
2.2.1 Horizontal Axis Wind Turbine (HAWT) 6
2.2.2 Vertical Axis Wind Turbines (VAWT) 7
2.2.2.1 Savonius VAWTs 9

CHAPTER 3: S DESIGN AND PROTOTYPE 13
3.1 Background Research 13
3.2 Design Blade Turbine 14
3.3 Experimental Setup 16
3.4 Measurements and Instrumentation 18

CHAPTER 4: RESULTS AND DISCUSSIONS 20
4.1 Effect of wind speed and Overlap for L =30 mm 20
4.2 Relationship between Average Static Torques with Wind speed for L =30 mm 24
4.3 Relationship between Average Static Torques with RPM for L =30 mm 28
4.4 Relationship between Average Powers with Wind Speed for L =30 mm 31
4.5 Relationship between Average Powers with RPM for L =30 mm 34
4.6 Effect of wind speed and Overlap for L =50 mm 37
4.7 Relationship between Average Static Torques with Wind speed for L =50 mm 41
4.8 Relationship between Average Static Torques with RPM for L =50 mm 44
4.9 Relationship between Average Powers with Wind Speed for L =50 mm 47
4.10 Relationship between Average Powers with RPM for L =50 mm 50
4.11 Comparison between L =30mm and L = 50 mm 53

CHAPTER 5: CONCLUSIONS AND FUTURE WORKS... 60
5.1 Conclusions.. 60
5.2 Future Works.. 60

REFERENCES.. 62

LIST OF TABLES

Table 2.1: Definition of classes of wind power density for 50 meter ……………….... 4
Table 3.1: Geometric parameters of unconventional Savonius turbine 16
Table 4.1: Average Static torques with respect to wind speed for L =30 mm 27
Table 4.2: Average Static torques with respect to RPM for L =30 mm 30
Table 4.3: Average power with respect to wind speed for L =30 mm 33
Table 4.4: Average power with respect to rotational speed (RPM) for L =30 mm 36
Table 4.5: Average static torque with respect to wind speed for L =50 mm 43
Table 4.6: Average static torque with respect to RPM for L =50 mm 46
Table 4.7: Average power with respect to wind speed for L =50 mm 49
Table 4.8: Average power with respect to RPM for L =50 mm 52

LIST OF FIGURES

Figure 2.1:	Horizontal axis wind turbine	6
Figure 2.2:	Key components of a horizontal-axis upwind turbine	7
Figure 2.3:	Different Types of VAWTs …………………………………………	8
Figure 2.4:	Two and three buckets Savonius VAWT	9
Figure 2.5:	Two vertical arrangements of two sets of Savonius rotors	10
Figure 2.6:	Two Buckets Savonius VAWT with different shapes	11
Figure 2.7:	Two buckets Savonius VAWT with curtains	11
Figure 2.8:	Two buckets Savonius VAWT with different overlap ratios	12
Figure 3.1:	Different arc bucket of Savonius rotors ……………………………	14
Figure 3.2:	Scheme of unconventional Savonius wind rotors	15
Figure 3.3:	Schematic view of experimental setup	17
Figure 3.4:	Procedure for calculating mechanical power of Savonius rotor …….	19
Figure 4.1:	The torque change -rotor angle at various wind speed with H =300 mm and t =3 mm	21
Figure 4.2:	The torque change - rotor angle at various wind speed with H =500 mm and t =3 mm	21
Figure 4.3:	The torque change -rotor angle at various wind speed with H =700 mm and t =3 mm	22
Figure 4.4:	The torque change- rotor angle at various wind speed with H =300 mm and t =6 mm	23
Figure 4.5:	The torque change- rotor angle at various wind speed with H =500 mm and t =6 mm	23
Figure 4.6:	The torque change-rotor angle at various wind speed with H =700 mm and t =6 mm	24
Figure 4.7:	Average torque change vs wind speed at different gap and blade thickness with H =300 mm	25
Figure 4.8:	Average torque change vs wind speed at different gap and blade thickness with H =500 mm	25
Figure 4.9:	Average torque change vs wind speed at different gap and blade thickness with H =700 mm	26
Figure 4.10:	Average torque change vs RPM at various gap and blade thickness with H =300 mm	28

Figure 4.11:	Average torque change vs RPM at various gap and blade thickness with H =500 mm	29
Figure 4.12:	Average torque change vs RPM at various gap and blade thickness with H =700 mm	29
Figure 4.13:	Average power change vs wind speed at various gap and blade thickness with H =300 mm	31
Figure 4.14:	Average power change vs wind speed at various gap and blade thickness with H =500 mm	32
Figure 4.15:	Average power change vs wind speed at various gap and blade thickness with H =700 mm	32
Figure 4.16:	Average power change vs RPM at various gap and blade thickness with H =300 mm	34
Figure 4.17:	Average power change vs RPM at various gap and blade thickness with H =500 mm	34
Figure 4.18:	Average power change vs RPM at various gap and blade thickness with H =700 mm	35
Figure 4.19:	The torque change -rotor angle at various wind speed with H =300 mm and t =3 mm for L=50 mm	37
Figure 4.20:	The torque change -rotor angle at various wind speed with H =500 mm and t =3 mm for L=50 mm	38
Figure 4.21:	The torque change -rotor angle at various wind speed with H =700 mm and t =3 mm for L=50 mm	38
Figure 4.22:	The torque change -rotor angle at various wind speed with H =300 mm and t =6 mm for L=50 mm	39
Figure 4.23:	The torque change -rotor angle at various wind speed with H =500 mm and t =6 mm for L=50 mm	40
Figure 4.24:	The torque change -rotor angle at various wind speed with H =700 mm and t =6 mm for L=50 mm	40
Figure 4.25:	Average torque change vs wind speed at different gap and blade thickness with H =300 mm for L =50 mm	41
Figure 4.26:	Average torque change vs wind speed at different gap and blade thickness with H =500 mm for L =50 mm	42
Figure 4.27:	Average torque change vs wind speed at different gap and blade thickness with H =700 mm for L =50 mm	42
Figure 4.28:	Average torque change vs RPM at different gap and blade thickness with H =300 mm for L =50 mm	44

Figure 4.29: Average torque change vs RPM at different gap and blade thickness with H =500 mm for L =50 mm 45

Figure 4.30: Average torque change vs RPM at different gap and blade thickness with H =700 mm for L =50 mm 45

Figure 4.31: Average power change vs wind speed at different gap and blade thickness with H =300 mm for L =50 mm 47

Figure 4.32: Average power change vs wind speed at different gap and blade thickness with H =500 mm for L =50 mm 48

Figure 4.33: Average power change vs wind speed at different gap and blade thickness with H =700 mm for L =50 mm 48

Figure 4.34: Average power change vs RPM at different gap and blade thickness with H =300 mm for L =50 mm 50

Figure 4.35: Average power change vs RPM at different gap and blade thickness with H =500 mm for L =50 mm 51

Figure 4.36: Average power change vs RPM at different gap and blade thickness with H =700 mm for L =50 mm 51

Figure 4.37: Comparison average torque between L = 30mm and 50mm for H =300 mm and e =20 mm 53

Figure 4.38: Comparison average torque between L = 30mm and 50mm for H =300 mm and e =26 mm 54

Figure 4.39: Comparison average power between L = 30mm and 50mm for H =300 mm and e =20 mm 54

Figure 4.40: Comparison average power between L = 30mm and 50mm for H =300 mm and e =26 mm 55

Figure 4.41: Comparison average torque between L = 30mm and 50mm for H =500 mm and e =20 mm 55

Figure 4.42: Comparison average torque between L = 30mm and 50mm for H =500 mm and e =26 mm 56

Figure 4.43: Comparison average power between L = 30mm and 50mm for H =500 mm and e =20 mm 56

Figure 4.44: Comparison average power between L = 30mm and 50mm for H =500 mm and e =26 mm 57

Figure 4.45: Comparison average torque between L = 30mm and 50mm for H =700 mm and e =20 mm 57

Figure 4.46: Comparison average torque between L = 30mm and 50mm for H =700 mm and e =26 mm 58

Figure 4.47: Comparison average power between L = 30mm and 50mm for H =700 mm and e =20 mm 58

Figure 4.48: Comparison average power between L = 30mm and 50mm for H =700 mm and e =26 mm 59

LIST OF SYMBOLS USED

C_p	Power coefficient, dimensionless
D	Diameter of rotor, mm
D_s	Shaft diameter, mm
e	Gap, mm
F	Force acting on the rotor shaft, N
g	Gravitational acceleration, m/s^2
H	Blade height, mm
H	New height, mm
H_0	Original height, mm
m	Mass loaded on the pan, kg
P	Power generation, Watt
R	Rotor radius, mm
r	Shaft radius, mm
s	Spring balance, kg
T	Torque, N.m
u_e	Maximum velocity, m/s
V	Wind speed, m/s
V_0	Wind speed at the original height, m/s
ρ	Air density, kg/m^3
λ	Tip speed ratio, dimensionless
ω	Rotational speed, rad/s
α	Surface roughness exponent, mm

CHAPTER 1
INTRODUCTION

1.1 Background of the study

Wind power has been used as long as humans have put sails into the wind. Wind turbine is a machine used to convert the wind energy into mechanical energy. There are two types of wind turbine which can be classified as horizontal axis wind turbine (HAWT) and vertical axis wind turbine (VAWT). Vertical axis wind turbine is independent of the wind direction (Gasch & Twele, 2012) and the rotating axis is perpendicular to the wind direction (Adaramola, 2014). Savonius wind turbine is a vertical axis wind turbine type and has a simple configuration and are able to work at low wind speed (Bhatti & Kothari, 2003). One of the main advantages of Savonius rotor has a higher torque compared to another types of vertical axis turbines (Menet, 2004). The Savonius wind turbine is suitable for local electricity production requiring low power, such as street-lighting systems in urban areas (Ricci et al., 2016; Ricci et al., 2014). Therefore, the project brief involves the design of new configuration of non-conventional a small scale of Savonius vertical axis wind turbine that can be easily mass produced and fitted to every household in Northern Cyprus to aid electricity consumption.

1.2 Research Goals

The aim of this thesis is to investigate the effect of blade geometries on the performance of unconventional Savonius vertical axis wind turbine. Therefore, the specific objectives of this work are:

1. Study the characteristic of static torque and mechanical power of unconventional Savonius wind rotors.
2. Study the impact of blade height on the mechanical power of the rotors at different rotor positions (rotor angle) and wind speed.
3. Study the impact of blade thickness on the mechanical power of the rotors at different rotor positions and wind speed.

1.3 Research Outline

This chapter presents a concise introduction to wind power and its importance for human life. In chapter 2, wind turbine background is discussed in details, followed by a discussion of the type of turbines, which are the main topic of this work. Chapter 3 illustrates the designed and procedure for calculating the static torque and mechanical power of the rotors. All the results of the experiments are presented in chapter 4 for unconventional Savonius rotors. The thesis ends with conclusions and suggestions for future work in chapter 5.

CHAPTER 2
WIND TURBINE BACKGROUND

As world population and standards of living increase there is an ever growing demand for energy. This increase in energy creates significant demand for energy created by fossil fuels, which the world has a limited amount of and carbon emissions can lead to global warming. The fears of diminishing natural resources and concern of significant climate change as a result of the burning of fossil fuels has created great worldwide interest in clean renewable energy that can meet the electrical demands of the world. One common strategy is to use wind turbines that generate electricity from wind.

2.1 Wind Introduction

Wind is generated from solar energy unevenly heating the earth. This uneven heating creates pressure changes in the atmosphere, generating wind. This wind can then be harnessed by a wind turbine. As the wind pushes the blades of a turbine, a generator attached to the axis of the shaft and when spun creates electricity that can be sent to the grid and used in households for electricity.

Wind turbines are a clean way to generate power, yet there are many significant problems with them as well (Ledec et al., 2011). One problem is that they are extremely expensive to design and install, and in order to generate enough energy for communities and cities require space for wind farms. Another issue is that they have to be created in locations where there is enough wind energy to generate enough electricity to justify the cost of the machine.

2.1.1 Wind Power Density

Wind power density, measured in watts per square meter of blade surface, is used to evaluate the wind resource available at a potential site (United States, 2000). The wind power density indicates how much energy is available for conversion by wind turbine (United States, 2000).

Geography can greatly affect wind speed, and in effect the power from the wind. Knowing this information prior to setting up a wind turbine is imperative. Calculating the average power from wind is a simple equation (Mani & Mooley, 1983; Gipe, 2003):

$$P = \frac{1}{2}\rho V^3 A \qquad (2.1)$$

Equation 2.1 indicates the importance of wind speed in power generation because power generation increases proportionally as wind increases to the third power. Knowing the power density will allow wind turbines to be placed in efficient locations for generating electricity. Table 2.1 shows a scale for power density using equation 1. Wind class four does not have sufficient wind power for large scale energy generation, yet it does potentially have value in personal wind turbine generation. Classes 5-7 have enough energy to be efficient in large scale wind turbine generation intended to wind power communities and cities.

Table 2.1: Definition of classes of wind power density for 50 meter (United States, 2000)

Wind power Class	**Wind power density [W/m^2]**	**Speed [m/s]**
4	400-500	7.0 – 7.5
5	500 – 600	7.5 – 8.0
6	600 – 800	8.0 – 8.8
7	> 800	> 8.8

2.1.2 Wind Speed

Another important factor is the height of the turbine rotor. One of the major reasons wind turbine costs are so high is because the higher altitude the turbine is located, the higher the velocity of the wind, which in turn increases the power output from the generator. Equation 2.2 is the power model which estimates the effect that height has on wind (Gipe, 1995).

$$V = V_0 \left[\frac{H}{H_0}\right]^{\alpha} \qquad (2.2)$$

Where V_0 is the wind speed at the original height, V is the wind weed at new height, H_0 is the original height, H is the new height and α is the surface roughness exponent.

2.1.3 Power Coefficient

The power coefficient of a wind energy (Rashid, 2007) is given by

$$C_p = \frac{\text{Mechanical power produced by wind turbine}}{\text{Avaiilable power in the wind}} \qquad 2.3$$

The power coefficient differs from the efficiency in the sense that the latter includes the losses in mechanical transmission, electrical generation, etc.(Bhadra et al., 2005), whereas the former is just the efficiency of conversion of wind energy into mechanical energy of the shaft. The maximum theoretically possible coefficient of power is called the Betz limit which is 0.593. Most current turbines today have a power coefficient between 0.3 and 0.4 (Paul, 2010).

2.1.4 Tip Speed Ratio

A wind energy converter is classified through the characteristic tip speed ratio (λ).This is the ratio (as a scalar) of the circumferential velocity of the rotor at the end of blade (maximum velocity, u_e) and the wind velocity (V_0) in front of the rotor (Wagner & Mathur, 2014). Equation 2.4 defines the tip speed ratio is the ratio of the tip speed of the blade divided by the wind speed. The equation for tip speed ratio is described below ((Wagner & Mathur, 2014) :

$$\lambda = \frac{u_e}{V_0} = \frac{\omega R}{V_0} \qquad (2.4)$$

where ω is the rotor rotational speed in radians per second and R is the rotor radius in meters.

2.2 Wind Turbine Classification

The two main classifications of wind turbines are horizontal axis wind turbine (HAWT) and vertical axis wind turbine (VAWT) (Hemami, 2012). The most common turbines are horizontal axis wind turbines. The rotating axis of these turbines is parallel to incoming flow.

2.2.1 Horizontal Axis Wind Turbine (HAWT)

The most common type of wind turbine is HAWTs, which work on the basic principle of lift (Rivkin et al., 2014). The rotating axis of turbines is parallel to the direction of incoming flow (Turner, 2005). The torque generated to rotate the turbine is produced as a result of the pressure difference on top and bottom surface of the wind turbine blade (Dinçer & Zamfirescu, 2012). Figure 2.1 shows HAWT with three blades.

(a) Commercial wind turbine (b) Small domestic scale wind turbine

Figure 2.1: Horizontal axis wind turbine (Wood, 2011)

In the top of the tower of horizontal axis wind turbine consists a rotor shaft and electrical generator (Rivkin et al., 2014). The main components for HAWTs (Harrison et al, 2000) as shown in Figure 2.2 are

- Blade rotor, which take out the kinetic energy present in the wind and convert it into mechanical power.
- The nacelle, with a power control system that limits and conditions the extracted power; a gear box that transfers the load and increases the speed of rotational to drive the generator; and an electrical system which converts the mechanical energy into electrical energy.
- A tower that supports the nacelle.

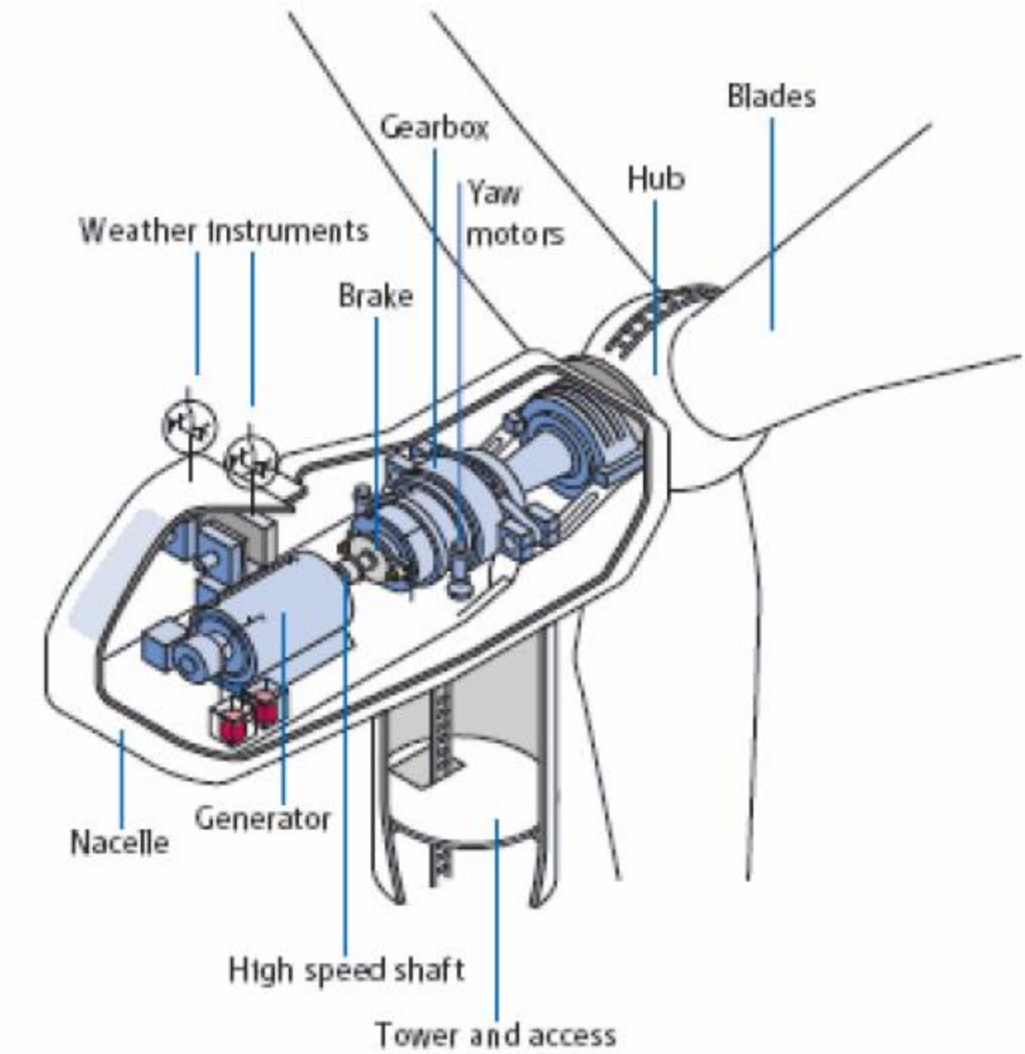

Figure 2.2: Key components of a horizontal-axis upwind turbine (npower renewables, 2007)

2.2.2 Vertical Axis Wind Turbines (VAWT)

The rotating axis of VAWT is perpendicular to the direction of the flow (Mathew, 2006). Key advantages of this arrangement are that the turbine does not need to be pointed into the wind to be effective. This is an advantage on sites where the wind direction is highly variable. VAWTs can utilize winds from varying directions (Wagner & Mathur, 2014).

Unlike HAWT, the electrical generator and gearbox of VAWT are placed near the ground, which it is more accessible for maintenance. Drag may be created when the blade rotates into the wind. Vertical axis wind turbine is classified into two types; drag type as Savonius and lift type as Darrieus (Eriksson et al., 2008) (see Figure 2.3).

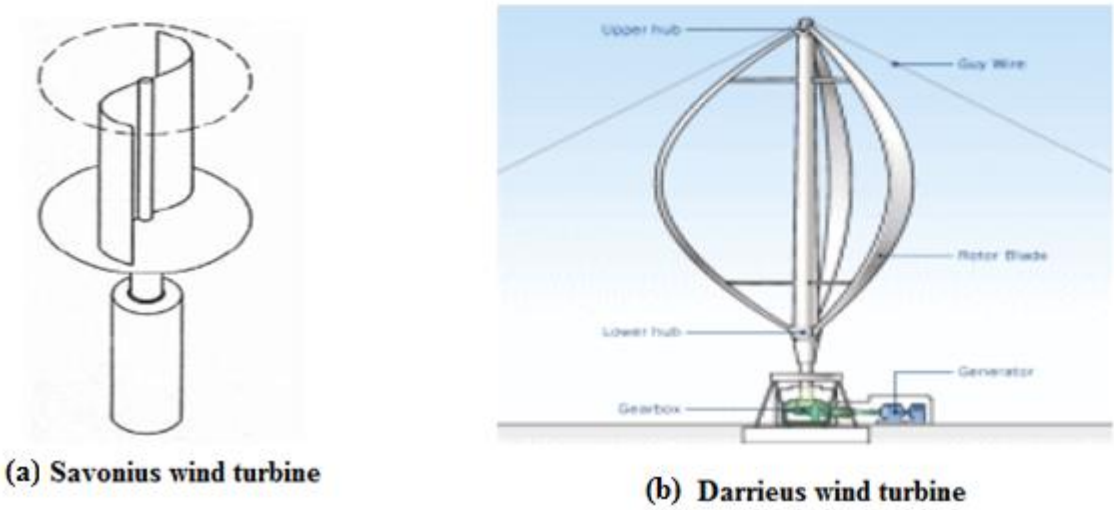

Figure 2.3: Different Types of VAWTs (Daut et al., 2012)

The main advantages of VAWTs over HAWTs are:

- Lower cut-in wind speed: VAWTs can start producing electricity at lower wind speeds compared to HAWTs which allows VAWTs to be placed closer to the ground.
- Omni-directional rotor: VAWTs do not need a pitch and yaw system to orient the blades into the wind.
- Lower noise level operation: VAWTs operate at lower tip speed ratios compared to HAWTs; they do not generate as much noise, and have lower vibration levels (Tong , 2010; Chiras et al., 2009).
- Lower construction, installation, and maintenance costs: Construction and installation costs are lower for VAWTs than HAWTs since VAWTs have fewer moving parts (Tong , 2010; Chiras et al., 2009).

- The inverter and generator are located near the ground and a gearbox may not be required (direct generation systems) making a VAWT easier to maintain (Tong, 2010; Chiras et al., 2009).

2.2.2.1 Savonius VAWTs

The Savonius wind turbine was invented 1929; it is the simplest of all wind turbines. The Savonius wind turbine is a drag-type turbine, which consists of two buckets or more buckets as shown in Figure 2.4. Because of the curvature, the buckets experience less drag when they move beside the wind (Retarding Bucket) than when moving with the wind (Advancing Bucket). The variation in drag force affects the Savonius rotor to rotate at low wind velocity. In the symmetric drag position the flow attached to the convex surface of the advancing bucket produces a low pressure region that pulls the blade into torque-adding direction (Ghosh & Prelas, 2011). Savonius turbines are not widely used because of their low efficiencies compared to other lift type VAWTs (efficiency of Savonius turbine is 15-20%, Darrieus turbine efficiency is 35%) (Howell et al., 2011; Shigetomi et al., 2011), however Savonius turbines have the advantages of simple construction and low noise levels (Shigetomi et al., 2011).

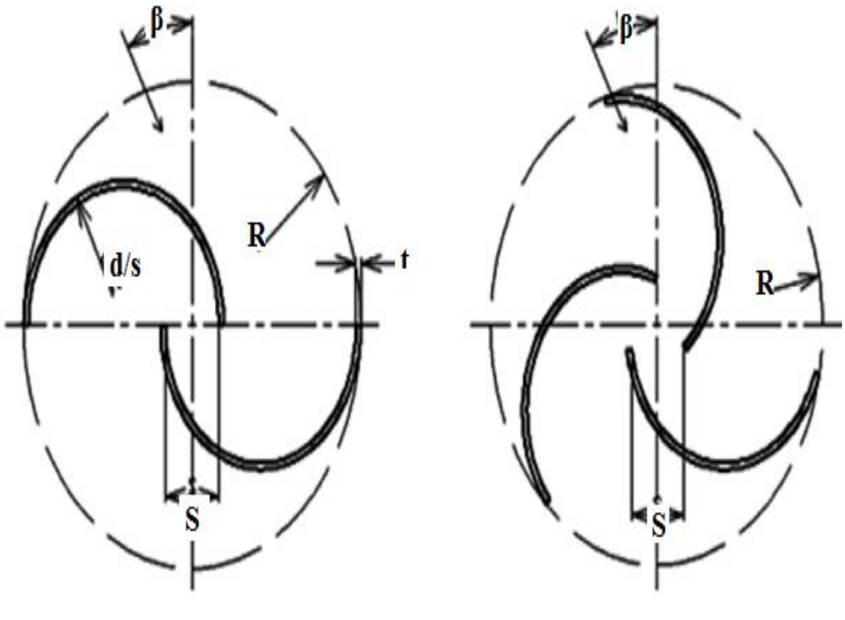

Figure 2.4: Two and Three Buckets Savonius VAWT (Ali, 2013)

Therefore, available in the literature are a lot of studies that have been conducted to increase the performance of a Savonius wind rotor. An increasing the performance of the Savonius rotor by changing blade numbers, material of the blade, overlap ratio and aspect ratio has been studied experimentally and numerically (Sheldahl et al. 1978; Altan et al., 2008a; Altan et al., 2008b) as shown 2.6, 2.7 and 2.8 . According to the pervious studied, the performance of two blades Savonius rotor is higher than three blades and the static torque of three blades is higher than two blades of rotors (Sheldahl et al. 1978). Setting two Savonius rotors in a vertical arrangement on the same shaft with a relative phase angle 90 degrees as shown in Figure 2.5, provides higher power output, higher stability of the auto start-up characteristics, and lower cyclic torsion during rotation (Sheldahl et al. 1978). The torque and the power coefficients of the Savonius rotor reach maximum values at an overlap ratio of 0.1-0.15 (Fujisawa, 1992).

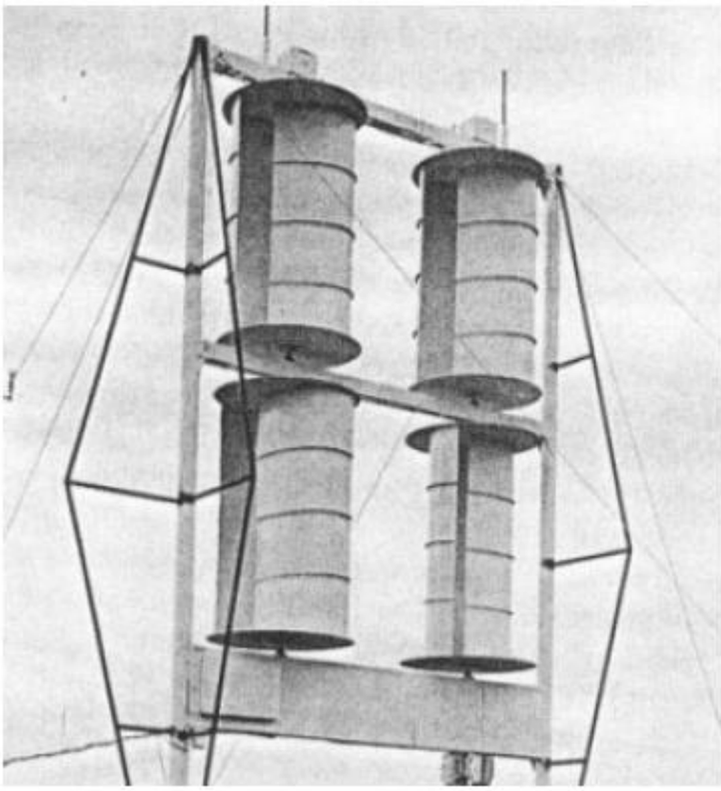

Figure 2.5: Two vertical arrangements of two sets of Savonius rotors (Sheldahl et al. 1978)

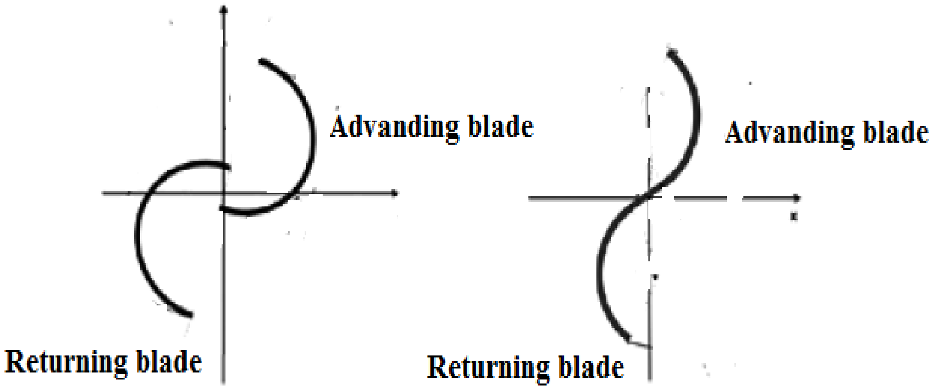

Figure 2.6: Two Buckets Savonius VAWT with different shapes (Altan et al., 2008)

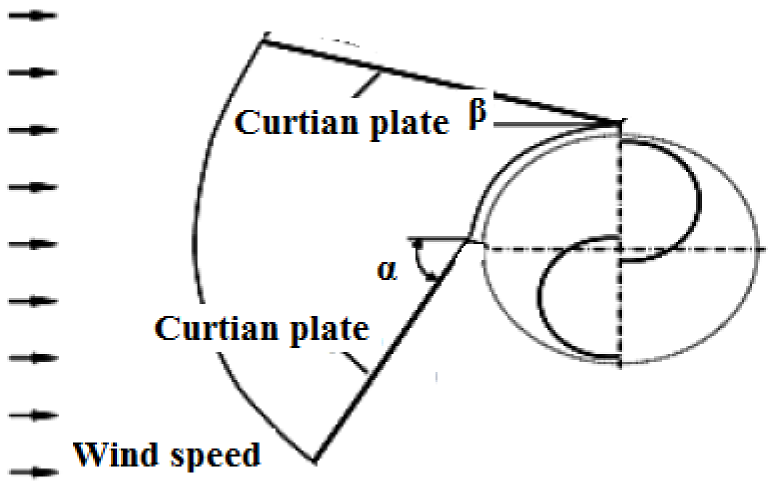

Figure 2.7: Two buckets Savonius VAWT with curtains (Altan et al., 2008)

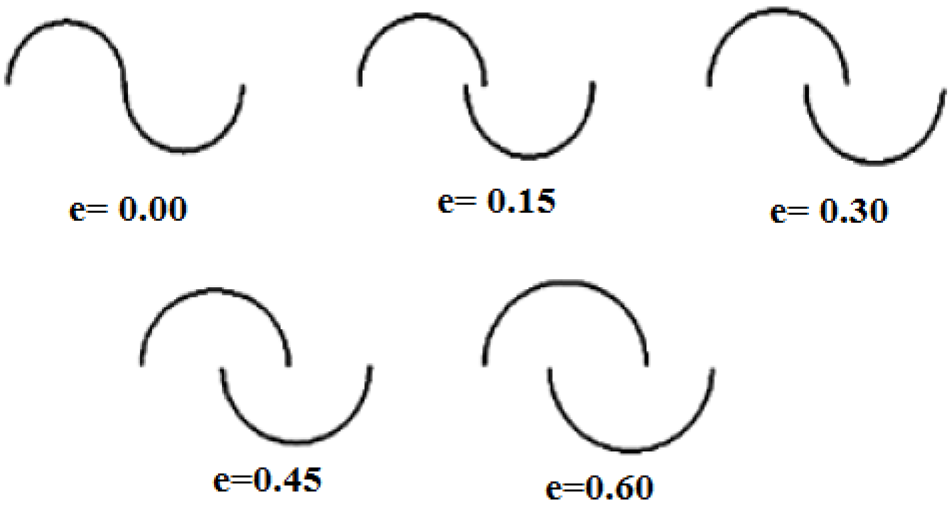

Figure 2.8: Two buckets Savonius VAWT with different overlap ratios (Fujisawa, 1992)

CHAPTER 3
DESIGN AND PROTOTYPE

This research aims to design unconventional Savonius wind rotors that could generate power under relatively high wind velocities. To carry out this goal, the objectives were to study the effect of blade geometries, wind speeds and rotor positions on the static torque and mechanical power of the rotors. To meet these objectives, the tasks were to:

- Complete with background research on conventional and non-conventional Savonius wind rotors,
- Design turbine blade designs for testing, and
- Create an experimental setup.

3.1 Background Research

Background research included reviewing a previous research, enclosed unconventional Savonius wind rotor by Driss et al. (2015). They studied numerically and experimentally the effect of bucket arc on the turbulent flow around unconventional Savonius wind rotors with keeping the other parameters (Figure 3.1) (blade height, blade thickness and blade number) constant. The results showed that as the bucket arc angle increases, the acceleration zone of the rotor will increase.

In this research, the effect of blade geometries and wind speed on static torque and mechanical power of unconventional Savonius rotors was discussed in this chapter.

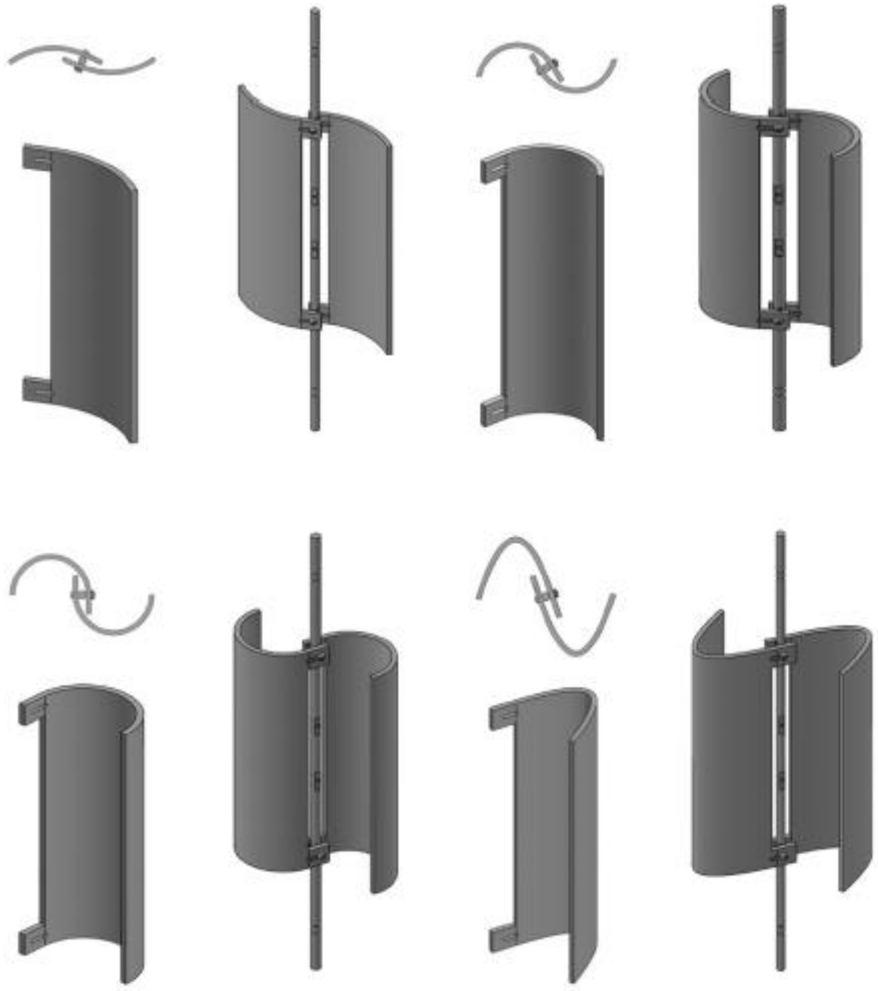

Figure 3.1: Different arc bucket of Savonius rotors (Driss et al., 2015)

3.2 Design Blade Turbine

The present experimental investigations are concerned with various geometries of unconventional Savonius wind rotors. This rotor is consisted by two half buckets characterized by various blade geometries as shown Figure 3.2. These geometries have different values of the following parameters: number of blades, aspect ratio (H/D), blade thickness (t), and overlap ratio (e/D) as shown in Table 3.1. The blades of rotors are made from light plastic (PVC) tubes with constant diameter (d = 150mm).

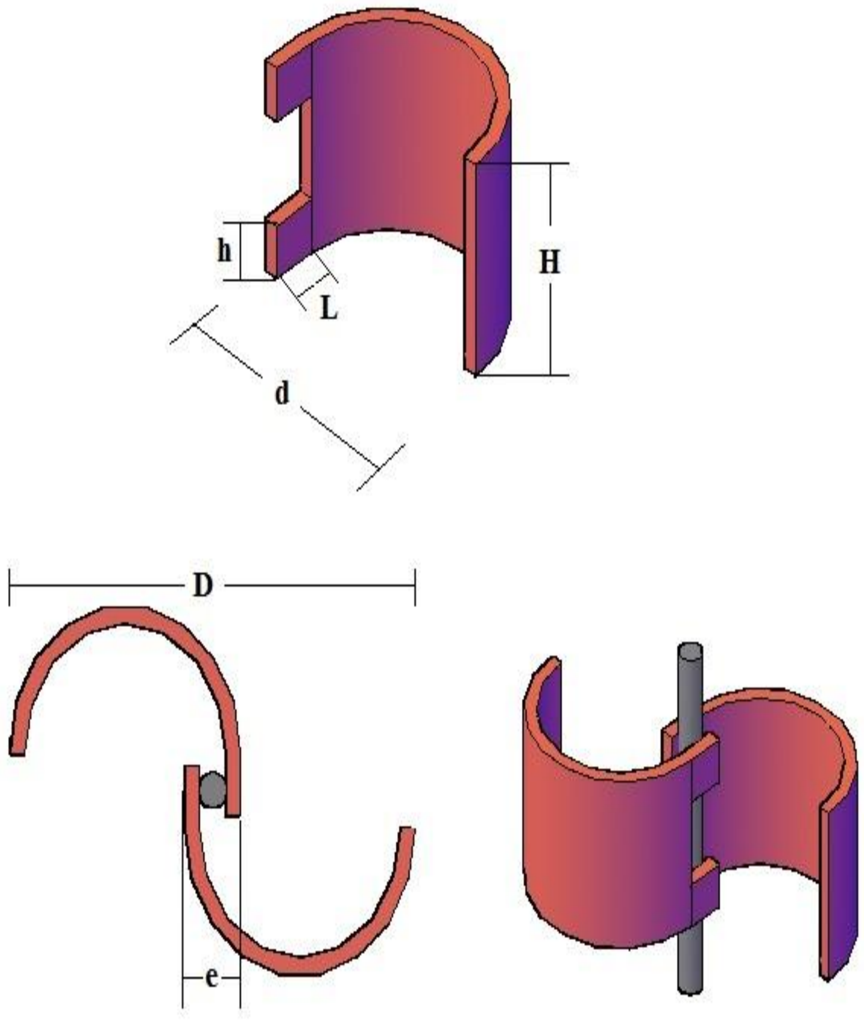

Figure 3.2: Scheme of unconventional Savonius wind rotors

Table 3.1: Geometric parameters of unconventional Savonius turbine

Designation of Savonius rotor	Diameter of shaft (D_s) [mm]	Diameter of rotor (D)	Height of rotor (H) [mm]	Gap (e) [mm]	Aspect ratio (H/D)	Overlap ratio (e/D)	Thickness of blade (t) [mm]
US#1	20	320	300	0	0.94	0	3
US#2	20	320	500	0	1.6	0	3
US#3	20	320	700	0	2.2	0	3
US#4	20	320	300	26	0.94	0.08	3
US#5	20	320	500	26	1.6	0.08	3
US#6	20	320	700	26	2.2	0.08	3
US#7	20	320	300	0	0.94	0	6
US#8	20	320	500	0	1.6	0	6
US#9	20	320	700	0	2.2	0	6
US#10	20	320	300	26	0.94	0.08	6
US#11	20	320	500	26	1.6	0.08	6
US#12	20	320	700	26	2.2	0.08	6
				Physical features			
Number of blade (N)				N = 2			
				Operational			
Rated wind speed (V) [m/s]				V = 3, 5, 7, 9, 11 and 13 m/s			
				Dimensional			
h [mm]				h = 70 mm			
L [mm]				L = 30 and 50 mm			

3.3 Experimental Setup

The experimental setup in the study was made according to previous study (Mahmoud et al., 2012; Kamoji et al., 2009). Figure 3.3 shows a representation diagram of the experimental set-up used in this work. As can be seen, the experimental set-up consists of three main parts which are the wind tunnel, rotor and measurement devices. The wind tunnel used in the experiments is an open-circuit type and has a squared exit (800 mm ×800 mm). Its wind velocity could also be changed with the use of an adjustable damper. The Savonius wind rotor and measurement devices have been installed away from the exit of this wind tunnel. Materials were selected to avoid structural failure of the wind turbine due to the forces that winds would impose on the blades. The drive shaft carried the most stress in this system due to the torsion produced by the blades. The Savonius rotor has been placed on a wood table. The shaft was made from galvanized steel. The blade rotors were made of PVC. Two ball bearings have been used to support the rotor shaft at top and bottom and to minimize the friction force. And then measurements of RPM, and wind velocity have been measured by RPM reader and pitot tube, respectively. Additionally, a centrifugal fan is used as the wind source for doing experiments. The wind velocity, V, was set at 3, 5, 7, 9, 11 and 13 m/s by adjusting the distance between the wind tunnel and the structure as shown in Figure 3.3.

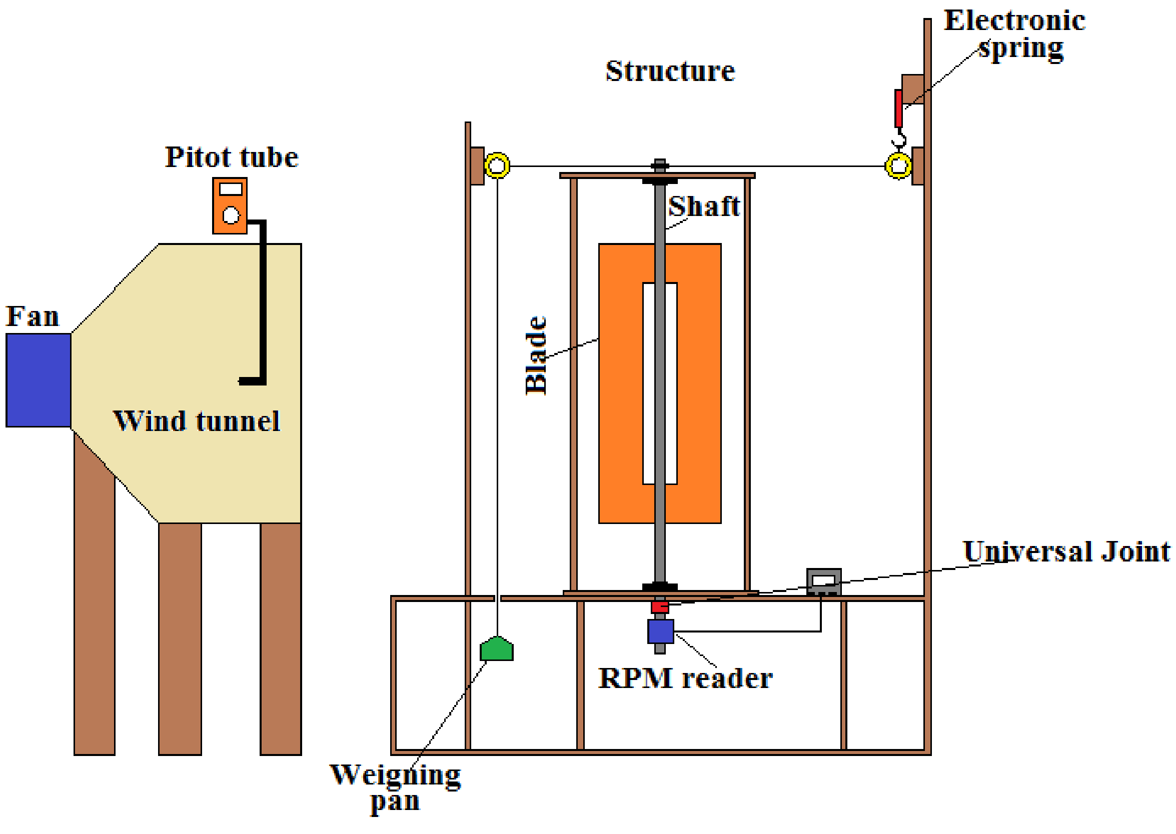

Figure 3.3: Schematic view of experimental setup

3.4 Measurements and Instrumentation

The mechanical power for unconventional Savonius rotors is estimated by multiplying the torque with angular speed at various wind speed and rotor positions. The arrangement used to do that is shown in Figure 3.3. It contains pulley system, nylon string, weighing pan and spring balance. The weighing pan, pulley and spring balance are connected by a nylon string of 1 mm diameter as shown in Figure 3.3. Pitot tube and RPM reader are used to measure the wind speed and rotational speed of the shaft, respectively. The rotor is loaded gradually to record spring balance reading, weights and rotational speed of the rotor. A set of tests are carried to calculate the static torque and mechanical power of the rotor at a given rotor angle using the brake drum measuring system. The static torque of the rotor is estimated at every 30° of the rotor angle. At a known wind velocity, the rotor is loaded to stop it from rotation at a given angle of rotor. The values of load and spring balance reading are recorded to calculate the static torque at a certain rotor angle

The mechanical power can be determined for each wind speed and rotor position as follow

$$P_m = T\omega \tag{3.1}$$

where T is the torque and ω is the angular speed. The angular speed is defined in rad/s as:

$$\omega = \frac{2\pi \text{ n}}{60} \tag{3.2}$$

where n is the shaft rotational speed in rpm. The mechanical torque is obtained in (N.m) by

$$T = Fr \tag{3.3}$$

where r is the shaft radius.

The force acting on the rotor shaft obtained in (N) by:

$$F = (m - s)g \tag{3.4}$$

where m is the mass loaded on the pan in kg, s is the spring balance reading in kg and g is the gravitational acceleration.

The procedures of torque and power calculation of unconventional Savonius vertical axis wind turbine can be described in Figure 3.4:

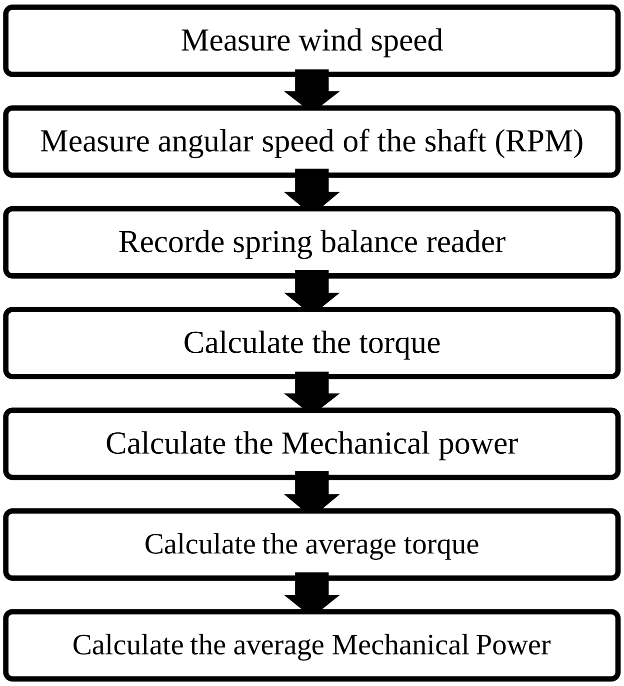

Figure 3.4: Procedure for calculating mechanical power of Savonius rotor

CHAPTER 4
RESULTS and DISCUSSIONS

The present experimental investigations are concerned with various geometries of rotors. The static torques of the rotors has been found at different rotor positions and wind speed. Then they have been compared through figures.

4.1 Effect of wind speed and overlap for L =30 mm

In this section the new blade shapes with L =30 mm for two different blade thickness (t = 3 mm and 6 mm) addressed in this work are presented and their main features are outlined.

a) Blade thickness (t = 3 mm)

Figure 4.1, 4.2 and 4.3 show the rotor angle-related changes of the static torque values obtained for different height (H = 300 mm, 500 mm and 700 mm) through experiments made at the various wind speed values of a between 3 and 13 m/s in step of 2 m/s. It is seen here that the static torque values obtained for blade height 700 mm are higher than the ones for 300 mm and 500 mm. The highest static torque values for the rotors have been found to be around rotor angle 0°, 180 and 360°. Moreover, it can be observed that the wind speeds lead to increase the value of static torque at various blade overlap and aspect ratio. It may be observed that the torque and power increase with the increase in the wind speed up to a maximum value. Unconventional Savonius rotor with overlap and aspect ratio of 0 and 0.94 respectively has the lowest torque and mechanical power among all the rotors covered in this study. Additionally, it found that static torque values decrease as the overlap ratio increases as shown in these figures. This may be due to the net drag force affected on rotor in blade thickness (t = 3 mm) case is higher than when blade thickness (t = 6 mm) case. As mention in chapter 3, Equation 3.4 represent the force that effect on the rotor, as spring reader increases with increase the weight of rotor. Since the mass loaded is constant which deepens on the blade geometries, the increasing spring balance reader leads to decrease the difference between mass loaded and spring balance reader, i.e. force acts on the rotor depends on the difference between mass loaded and spring balance reader. It can be noticed that as overlap increases the torque and mechanical power of the rotors decrease.

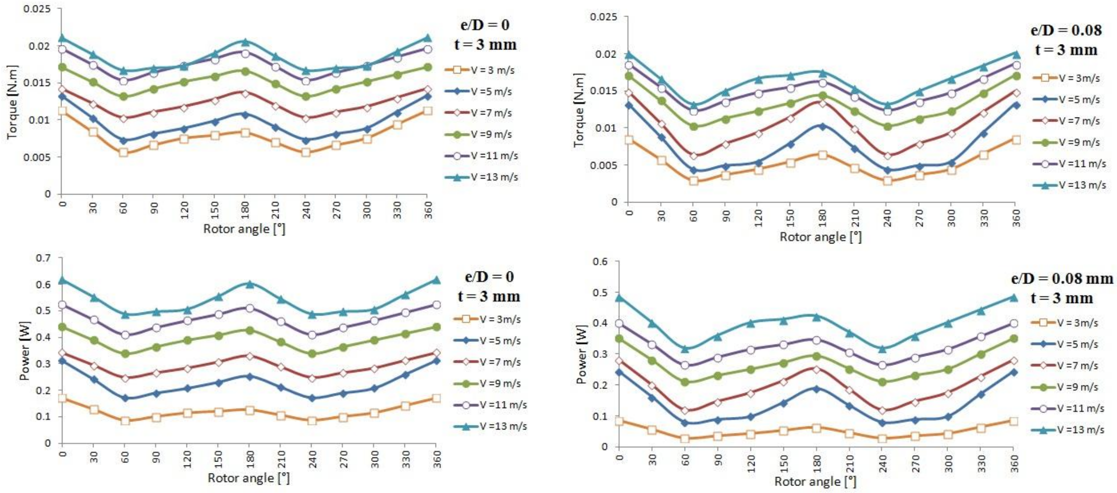

Figure 4.1: The torque change -rotor angle at various wind speed with aspect ratio of 0.94 and t =3 mm

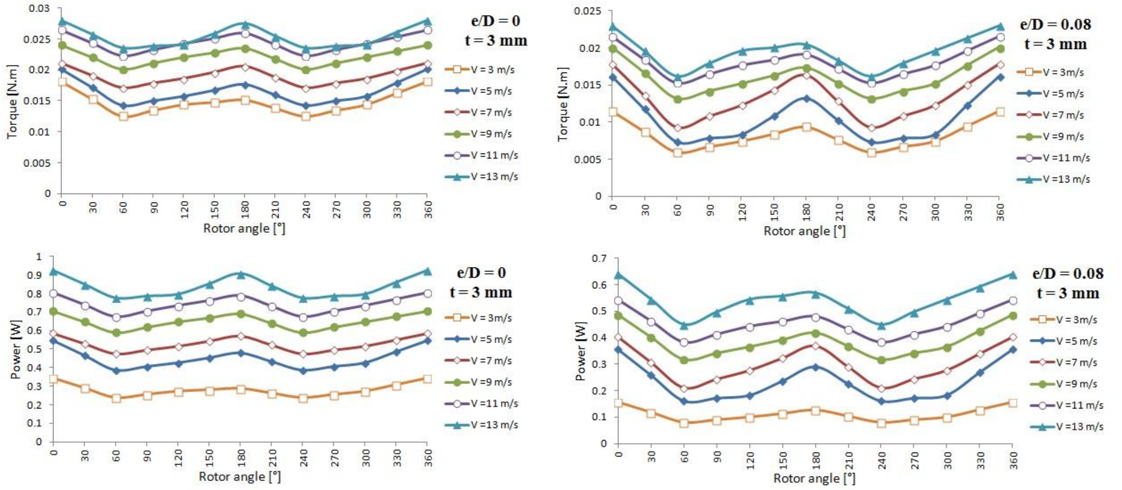

Figure 4.2: The torque change - rotor angle at various wind speed with aspect ratio of 1.6 and t =3 mm

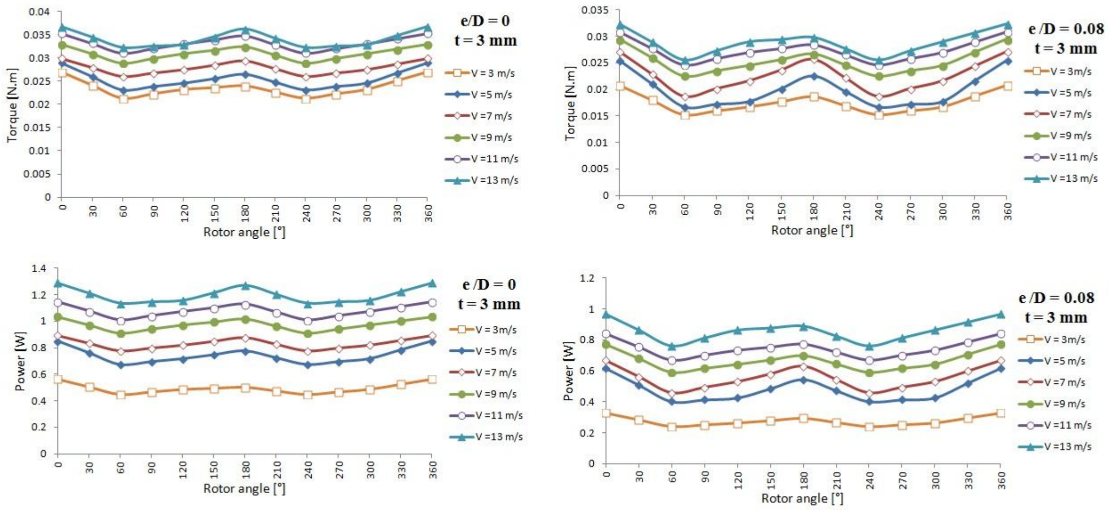

Figure 4.3: The torque change - rotor angle at various wind speed with aspect ratio of 2.2 and t =3 mm

b) Blade thickness (t = 6 mm)

Unconventional Savonius rotor with blade thickness 6 mm is tested at different wind velocities of 3 m/s, 5 m/s, 7 m/s, 9 m/s, 11 m/s and 13 m/s. Figures 4.4, 4.5 and 4.6 show the variation of torque and mechanical power for unconventional rotors with an aspect ratio of 0.94, 1.6 and 2.2 and overlap ratio of 0, and 0.08 at different various wind speeds. It can be seen that the rotor with aspect ratio 2.2 and overlap ratio 0.0 has the highest static torque compared to other rotors.

Furthermore, it observed here that the rotor without overlap gives higher torque and mechanical power than rotors with overlap.

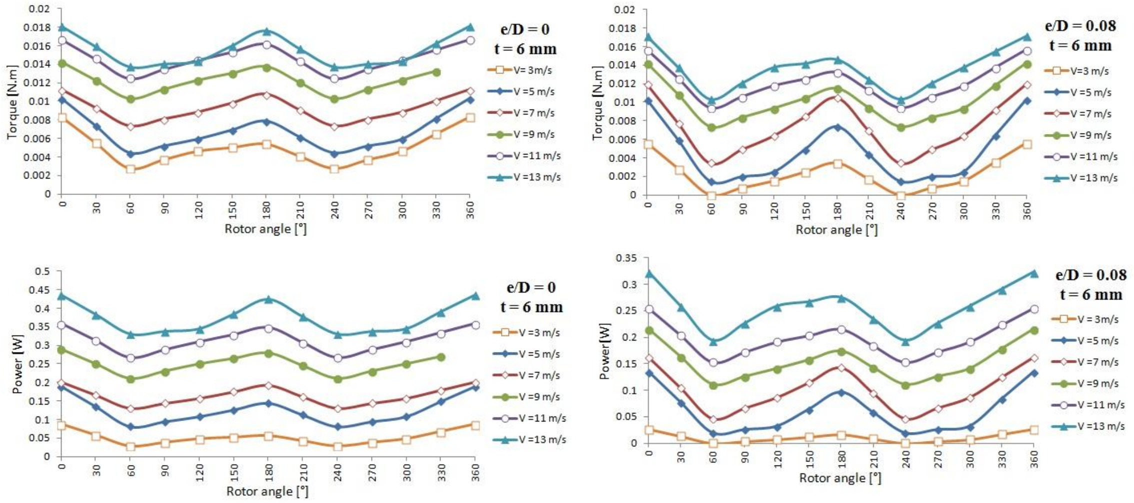

Figure 4.4: The torque change -rotor angle at various wind speed with aspect ratio of 0.94 and t =6 mm

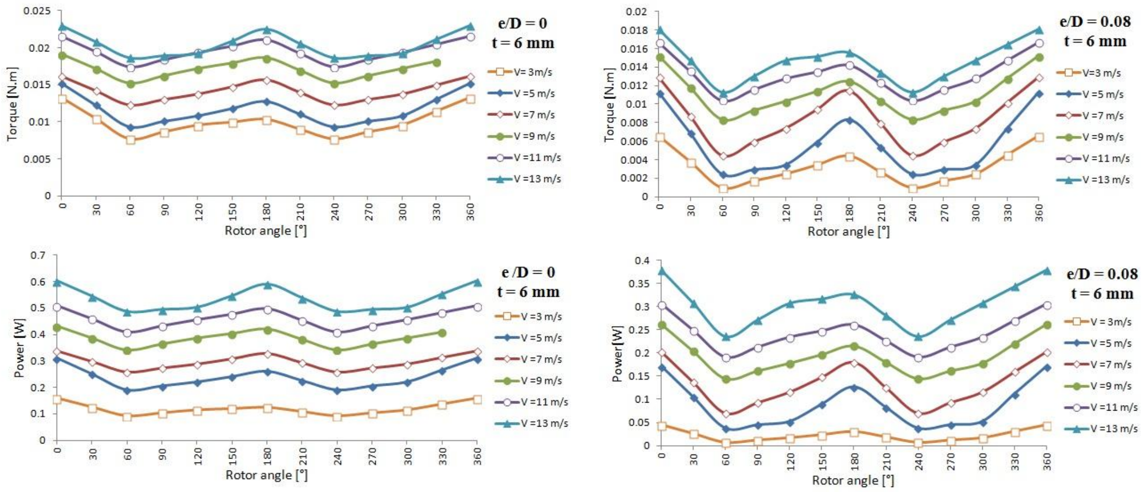

Figure 4.5: The torque change -rotor angle at various wind speed with aspect ratio of 1.6 and t =6 mm

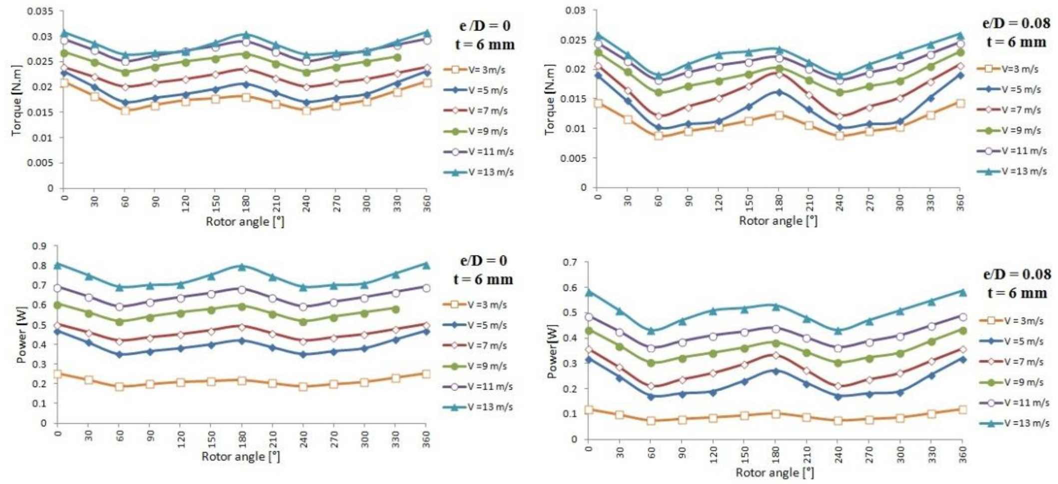

Figure 4.6: The torque change -rotor angle at various wind speed with aspect ratio of 2.2 and t =6 mm

4.2 Relationship between Average Static Torques with Wind speed for L =30 mm

The average static torque ($T_{average}$) is calculated by dividing the sum of all values of static torque at a different rotor angle by a number of the values. It is given by the formula

$$T_{average} = \frac{\sum_{i=1}^{n} T_i}{n} \tag{4.1}$$

Figures 4.7, 4.8 and 4.9 show the relation between average static torques and wind speed for different overlaps ratio and blade thickness. Also, they are summarized in Table 4.1. It can be seen that the average static torques increase when the blade height increases, blade thickness and overlap decrease. Moreover, the increasing wind speed leads to increase the average torque of rotors. It is clear here that there is an increase in average static torque with the rise in blade height and wind speed and decrease blade thickness and gap.

Moreover, it can be observed from Figures 4.7, 4.8 and 4.9 that the torque or mechanical powers of the rotor are inversely proportional to blade thickness i.e. the torque or mechanical power increase when blade thickness decreases. In addition, as aspect ratio increases the toque and mechanical power of the rotors increase. This may be due to the force affected on rotor in blade height 700 mm case is higher than those for blade height 500 mm and 300 mm cases.

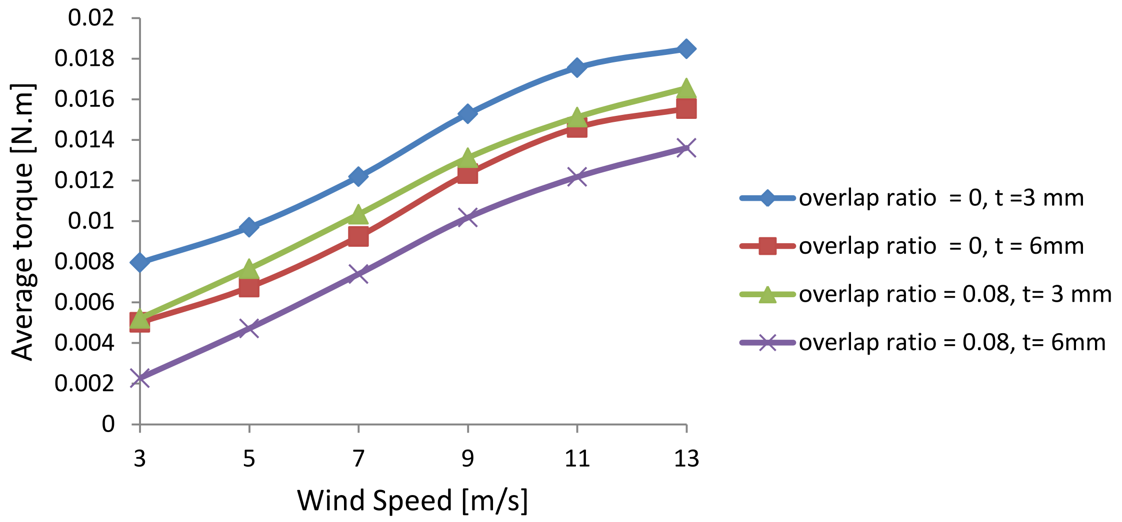

Figure 4.7: Average torque change vs wind speed at different overlap ratio and blade thickness with aspect ratio of 0.94

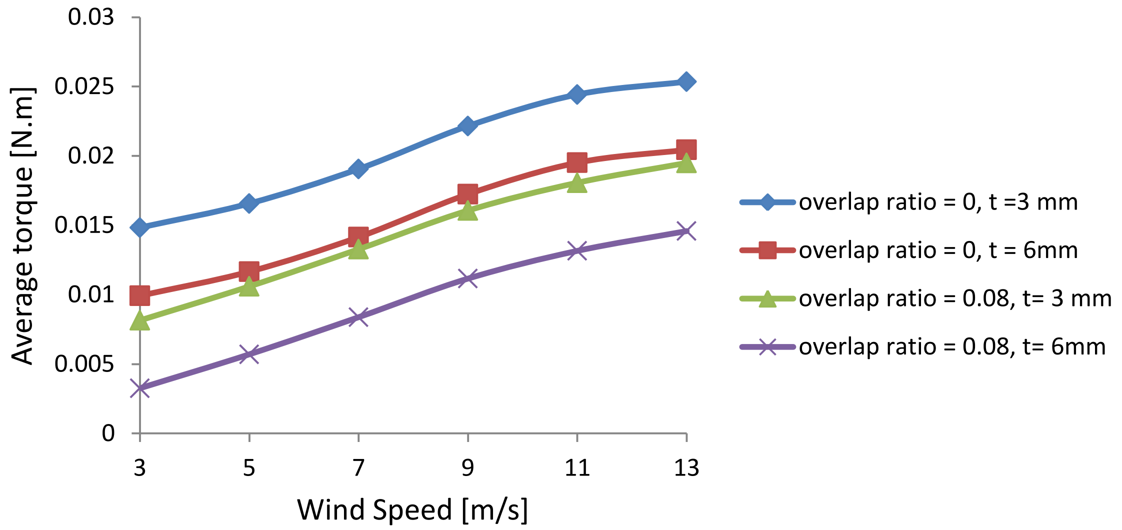

Figure 4.8: Average torque change vs wind speed at different overlap ratio and blade thickness with aspect ratio of 1.6

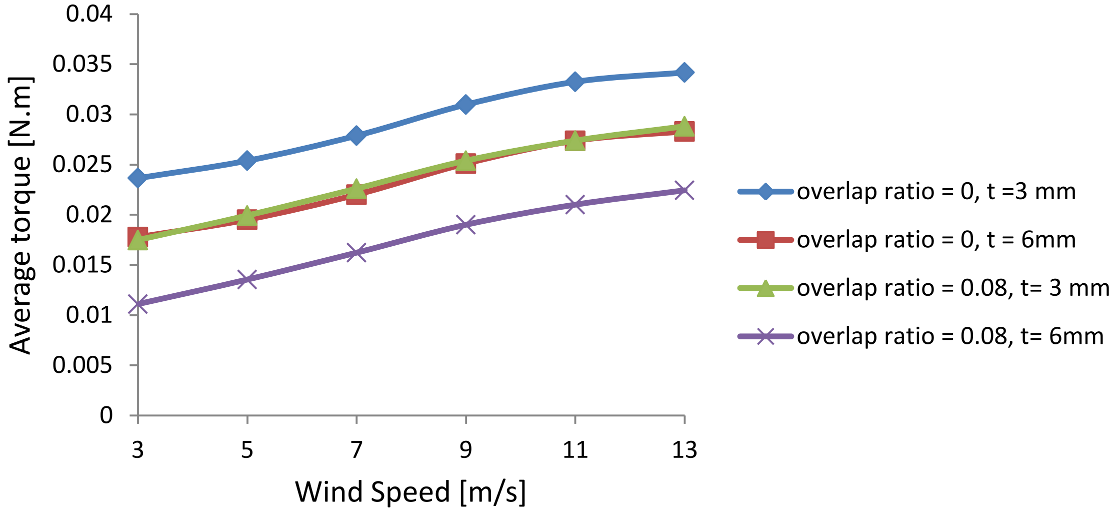

Figure 4.9: Average torque change vs wind speed at different overlap ratio and blade thickness with aspect ratio of 2.2

Table 4.1: Average Static torques with respect to wind speed for L =30 mm

Aspect ratio = 0.94, overlap ratio = 0.0, t = 3 mm						
Wind speed [m/s]	3	5	7	9	11	13
Average torque[N.m]	0.007961	0.009697	0.012187	0.015281	0.017552	0.018481
Aspect ratio = 0.94, overlap ratio = 0.0, t = 6 mm						
Wind speed [m/s]	3	5	7	9	11	13
Average torque[N.m]	0.005018	0.006754	0.009244	0.012338	0.014609	0.015538
Aspect ratio = 0.94, overlap ratio = 0.08, t = 3 mm						
Wind speed [m/s]	3	5	7	9	11	13
Average torque[N.m]	0.005214	0.007659	0.010338	0.013123	0.015122	0.016549
Aspect ratio = 0.94, overlap ratio = 0.08, t = 6 mm						
Wind speed [m/s]	3	5	7	9	11	13
Average torque[N.m]	0.002271	0.004716	0.007395	0.01018	0.012179	0.013606
Aspect ratio = 1.6, overlap ratio = 0.0, t = 3 mm						
Wind speed [m/s]	3	5	7	9	11	13
Average torque[N.m]	0.014828	0.016564	0.019054	0.022148	0.024419	0.025348
Aspect ratio = 1.6, overlap ratio = 0.0, t = 6 mm						
Wind speed [m/s]	3	5	7	9	11	13
Average torque[N.m]	0.009923	0.011659	0.014149	0.017243	0.019514	0.020443
Aspect ratio = 1.6, overlap ratio = 0.08, t = 3 mm						
Wind speed [m/s]	3	5	7	9	11	13
Average torque[N.m]	0.008157	0.010602	0.013281	0.016066	0.018065	0.019492
Aspect ratio = 1.6, overlap ratio = 0.08, t = 6 mm						
Wind speed [m/s]	3	5	7	9	11	13
Average torque[N.m]	0.003252	0.005697	0.008376	0.011161	0.01316	0.014587
Aspect ratio = 2.2, overlap ratio = 0.0, t = 3 mm						
Wind speed [m/s]	3	5	7	9	11	13
Average torque[N.m]	0.023657	0.025393	0.027883	0.030977	0.033248	0.034177
Aspect ratio = 2.2, overlap ratio = 0.0, t = 6 mm						
Wind speed [m/s]	3	5	7	9	11	13
Average torque[N.m]	0.017771	0.019507	0.021997	0.025091	0.027362	0.028291
Aspect ratio = 2.2, overlap ratio = 0.08, t = 3 mm						
Wind speed [m/s]	3	5	7	9	11	13
Average torque[N.m]	0.017477	0.019922	0.022601	0.025385	0.027385	0.028811
Aspect ratio = 2.2, overlap ratio = 0.08, t = 6 mm						
Wind speed [m/s]	3	5	7	9	11	13
Average torque[N.m]	0.0111	0.013545	0.016224	0.019009	0.021008	0.022435

4.3 Relationship between Average Static Torques with RPM for L =30 mm

Different rotors with various aspect ratios of 0.49, 1.6 and 2.2 are studied experimentally at variable values of RPM, overlap ratio and blade thickness. Figures 4.10, 4.11, 4.12 and Table 4.2 present the variation of average static torque with RPM for the different tested gaps and blade thickness. It is clear here that there is an increase in average static torque with the rise in RPM. At constant aspect ratio, when the torque of the rotor increases, the rotational speed, RPM, increases as overlap ratio and blade thickness decrease as shown in Figures 4.10, 4.11, 4.12 and Table 4.2.

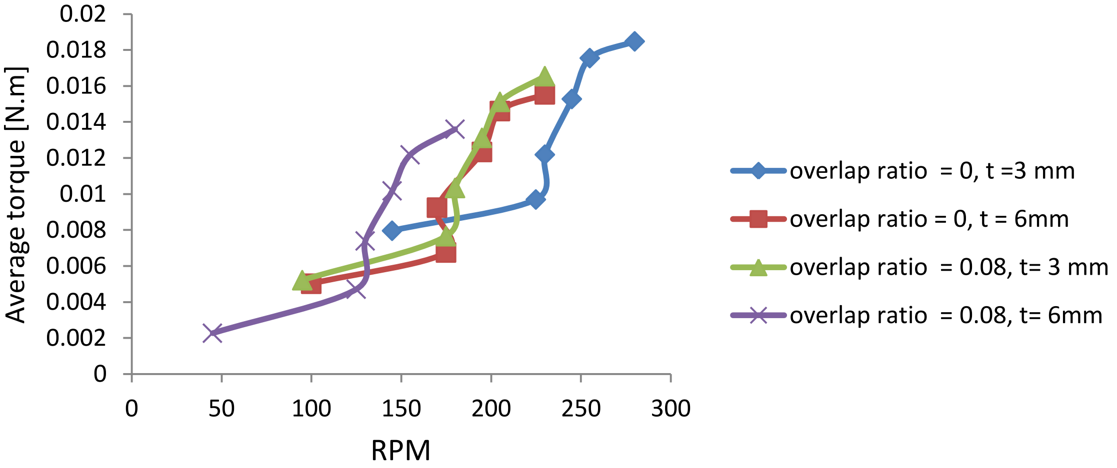

Figure 4.10: Average torque change vs RPM at various overlap ratio and blade thickness with aspect ratio of 0.94

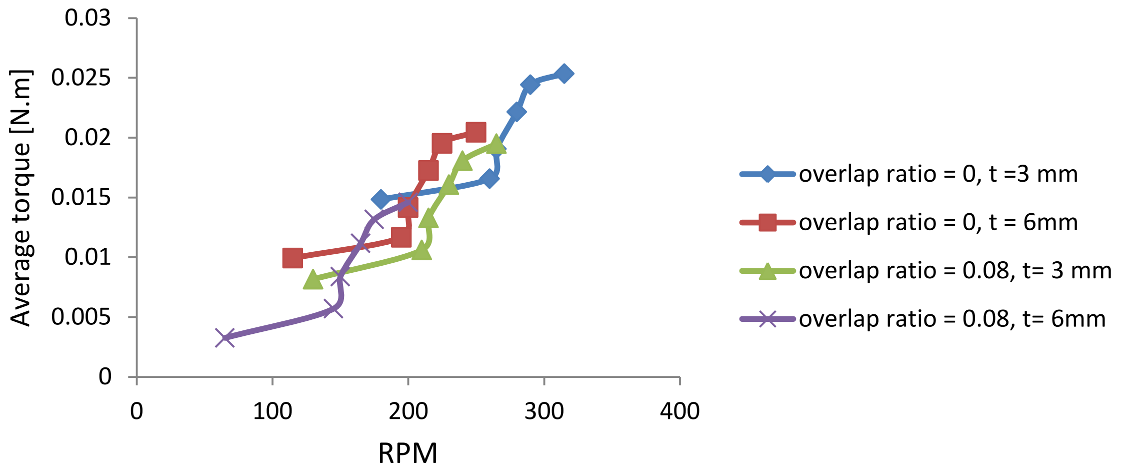

Figure 4.11: Average torque change vs RPM at various overlap ratio and blade thickness with aspect ratio of 1.6

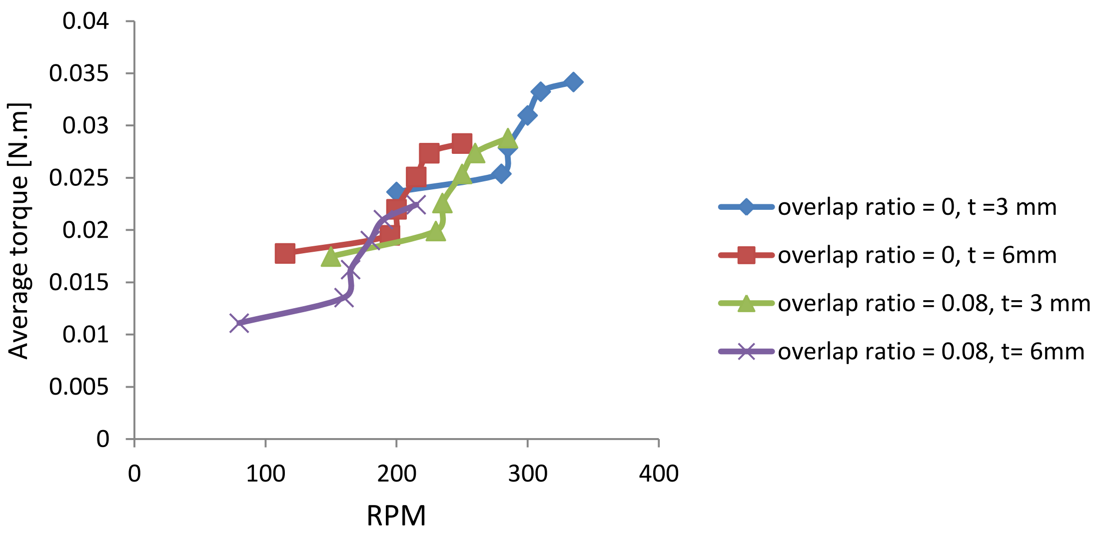

Figure 4.12: Average torque change vs RPM at various overlap ratio and blade thickness with aspect ratio of 2.2

Table 4.2: Average Static torques with respect to rotational speed (RPM) for L =30 mm

Aspect ratio = 0.49, overlap ratio = 0.0, t = 3 mm						
RPM	145	225	230	245	255	280
Average torque[N.m]	0.007961	0.009697	0.012187	0.015281	0.017552	0.018481
Aspect ratio = 0.49, overlap ratio = 0.0, t = 6 mm						
RPM	100	175	170	195	205	230
Average torque[N.m]	0.005018	0.006754	0.009244	0.012338	0.014609	0.015538
Aspect ratio = 0.49, overlap ratio = 0.08, t = 3 mm						
RPM	95	175	180	195	205	230
Average torque[N.m]	0.005214	0.007659	0.010338	0.013123	0.015122	0.016549
Aspect ratio = 0.49, overlap ratio = 0.08, t = 6 mm						
RPM	45	125	130	145	155	180
Average torque[N.m]	0.002271	0.004716	0.007395	0.01018	0.012179	0.013606
Aspect ratio = 1.6, overlap ratio = 0.0, t = 3 mm						
RPM	**180**	260	265	280	290	315
Average torque[N.m]	**0.014828**	0.016564	0.019054	0.022148	0.024419	0.025348
Aspect ratio = 1.6, overlap ratio = 0.0, t = 6 mm						
RPM	**115**	195	200	215	225	250
Average torque[N.m]	**0.009923**	0.011659	0.014149	0.017243	0.019514	0.020443
Aspect ratio = 1.6, overlap ratio = 0.08, t = 3 mm						
RPM	**130**	210	215	230	240	265
Average torque[N.m]	**0.008157**	0.010602	0.013281	0.016066	0.018065	0.019492
Aspect ratio = 1.6, overlap ratio = 0.08, t = 6 mm						
RPM	**65**	145	150	165	175	200
Average torque[N.m]	**0.003252**	0.005697	0.008376	0.011161	0.01316	0.014587
Aspect ratio = 2.2, overlap ratio = 0.0, t = 3 mm						
RPM	**200**	280	285	300	310	335
Average torque[N.m]	**0.023657**	0.025393	0.027883	0.030977	0.033248	0.034177
Aspect ratio = 2.2, overlap ratio = 0.0, t = 6 mm						
RPM	**115**	195	200	215	225	250
Average torque[N.m]	**0.017771**	0.019507	0.021997	0.025091	0.027362	0.028291
Aspect ratio = 2.2, overlap ratio = 0.08, t = 3 mm						
RPM	**150**	230	235	250	260	285
Average torque[N.m]	**0.017477**	0.019922	0.022601	0.025385	0.027385	0.028811
Aspect ratio = 2.2, overlap ratio = 0.08, t = 6 mm						
RPM	**80**	160	165	180	190	215
Average torque[N.m]	**0.0111**	0.013545	0.016224	0.019009	0.021008	0.022435

4.4 Relationship between Average Powers with Wind Speed for L =30 mm

The average mechanical power ($MP_{average}$) is calculated by dividing the sum of all values of mechanical power at a different rotor angle by a number of the values. It is given by the formula

$$MP_{average} = \frac{\sum_{i=1}^{n} MP_i}{n} \tag{4.2}$$

Effect of blade thickness and gaps is studied here for different rotors at various values of wind speed. The aspect ratio of 2.2, and blade thickness ,t = 3mm, of the rotor gives higher average power than parameters as shown in Figure 4.13, 4.14, 4.15 and Table 4.3. However, the average power is proportional to wind speed and aspect ratio and inversely proportional to overlap ratio. At constant aspect ratio and wind speed, when the overlap ratio increases, the power of the rotor will decrease as show in Figures 4.13, 4.14, 4.15 and Table 4.3.

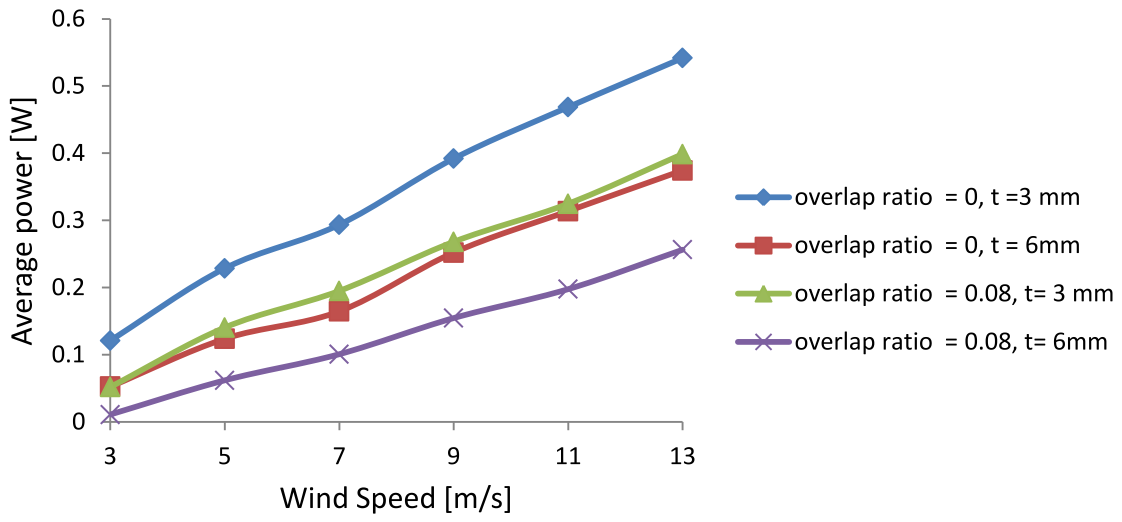

Figure 4.13: Average power change vs wind speed at various overlap ratio and blade thickness with aspect ratio of 0.94

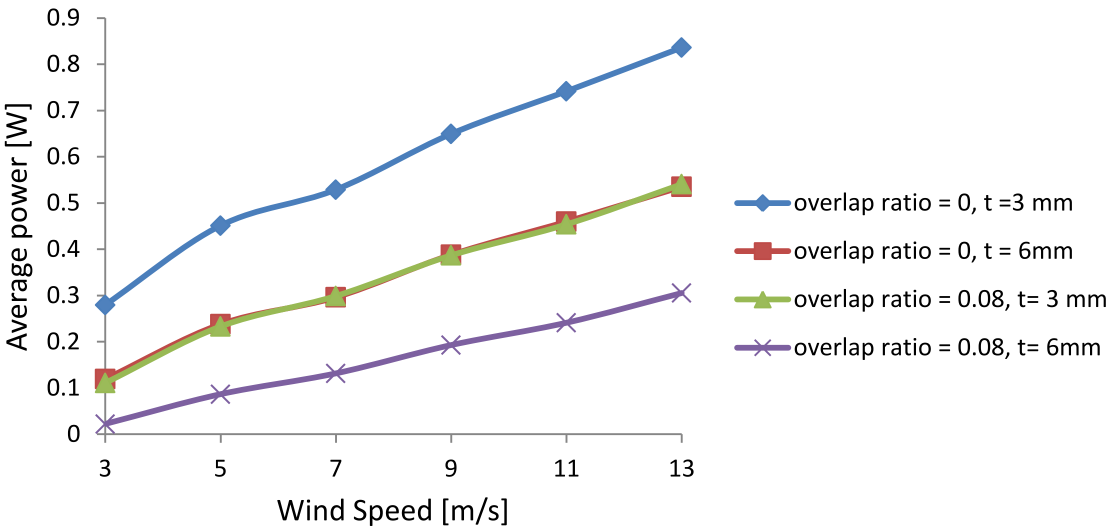

Figure 4.14: Average power change vs wind speed at various overlap ratio and blade thickness with aspect ratio of 1.6

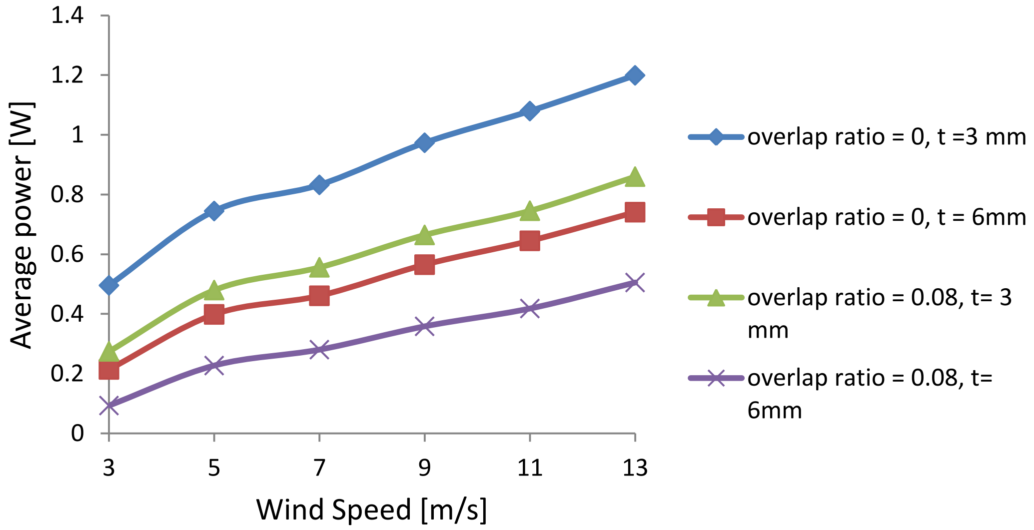

Figure 4.15: Average power change vs wind speed at various overlap ratio and blade thickness with aspect ratio of 2.2

Table 4.3: Average power with respect to wind speed for L =30 mm

Aspect ratio = 0.94, overlap ratio = 0.0, t = 3 mm						
Wind speed [m/s]	3	5	7	9	11	13
Average Power [W]	0.120882	0.228469	0.293523	0.392042	0.468696	0.541861
Aspect ratio = 0.94, overlap ratio = 0.0, t = 6 mm						
Wind speed [m/s]	3	5	7	9	11	13
Average Power [W]	0.052549	0.123766	0.164561	0.251938	0.313618	0.374219
Aspect ratio = 0.94, overlap ratio = 0.08, t = 3 mm						
Wind speed [m/s]	3	5	7	9	11	13
Average Power [W]	0.051873	0.140361	0.194865	0.267964	0.324633	0.398573
Aspect ratio = 0.94, overlap ratio = 0.08, t = 6 mm						
Wind speed [m/s]	3	5	7	9	11	13
Average Power [W]	0.010703	0.061735	0.100673	0.154569	0.197686	0.256454
Aspect ratio = 1.6, overlap ratio = 0.0, t = 3 mm						
Wind speed [m/s]	3	5	7	9	11	13
Average Power [W]	0.279497	0.450972	0.528748	0.649393	0.741563	0.836107
Aspect ratio = 1.6, overlap ratio = 0.0, t = 6 mm						
Wind speed [m/s]	3	5	7	9	11	13
Average Power [W]	0.119499	0.23807	0.296328	0.388209	0.459783	0.535168
Aspect ratio = 1.6, overlap ratio = 0.08, t = 3 mm						
Wind speed [m/s]	3	5	7	9	11	13
Average Power [W]	0.111048	0.233151	0.299015	0.386941	0.454022	0.540893
Aspect ratio = 1.6, overlap ratio = 0.08, t = 6 mm						
Wind speed [m/s]	3	5	7	9	11	13
Average Power [W]	0.022138	0.086508	0.13157	0.192838	0.241172	0.305494
Aspect ratio = 2.2, overlap ratio = 0.0, t = 3 mm						
Wind speed [m/s]	3	5	7	9	11	13
Average Power [W]	0.49546	0.744534	0.832148	0.973141	1.079314	1.198916
Aspect ratio = 2.2, overlap ratio = 0.0, t = 6 mm						
Wind speed [m/s]	3	5	7	9	11	13
Average Power [W]	0.214008	0.398324	0.460691	0.5649	0.644691	0.740623
Aspect ratio = 2.2, overlap ratio = 0.08, t = 3 mm						
Wind speed [m/s]	3	5	7	9	11	13
Average Power [W]	0.479814	0.556168	0.664565	0.745593	0.859849	0.923412
Aspect ratio = 2.2, overlap ratio = 0.08, t = 6 mm						
Wind speed [m/s]	3	5	7	9	11	13
Average Power [W]	0.092992	0.226948	0.280326	0.358296	0.417988	0.505097

4.5 Relationship between Average Powers with RPM for L =30 mm

Figures 4.16, 4.17 and 4.18 illustrate the variation in average power with RPM for the investigated rotors. Additionally, Table 4.4 compares the average power values of rotors with respects to wind speed and different blade height, thickness and gap. The results concluded that the average power increase with increasing the blade height and decreasing gap and blade thickness.

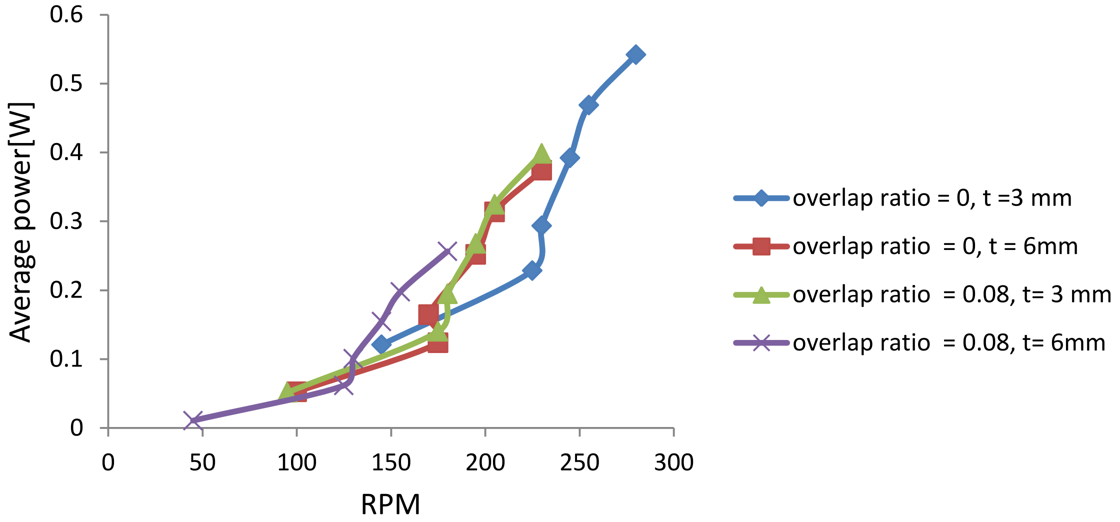

Figure 4.16: Average power change vs RPM at various overlap ratio and blade thickness with aspect ratio of 0.94

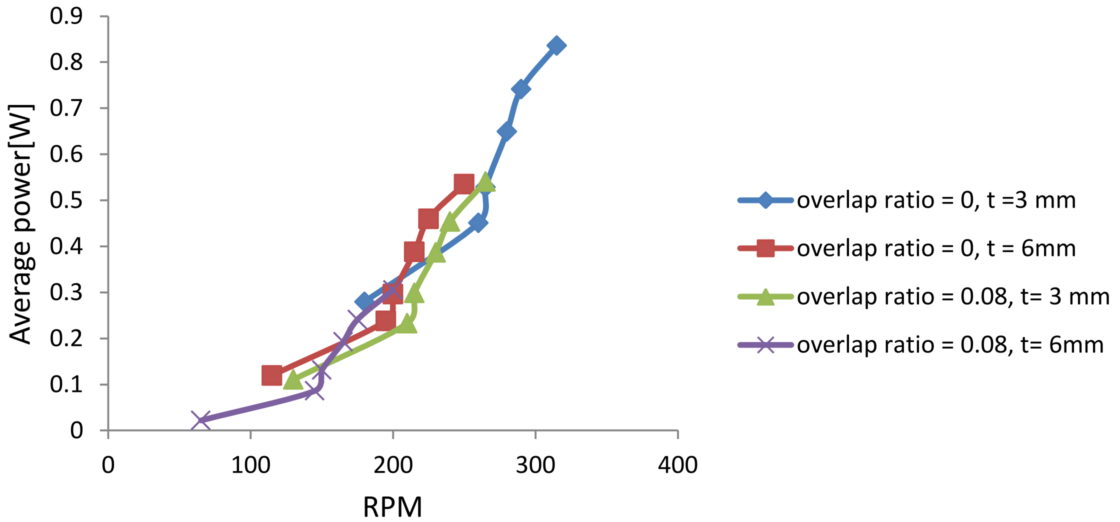

Figure 4.17: Average power change vs RPM at various overlap ratio and blade thickness with aspect ratio of 1.6

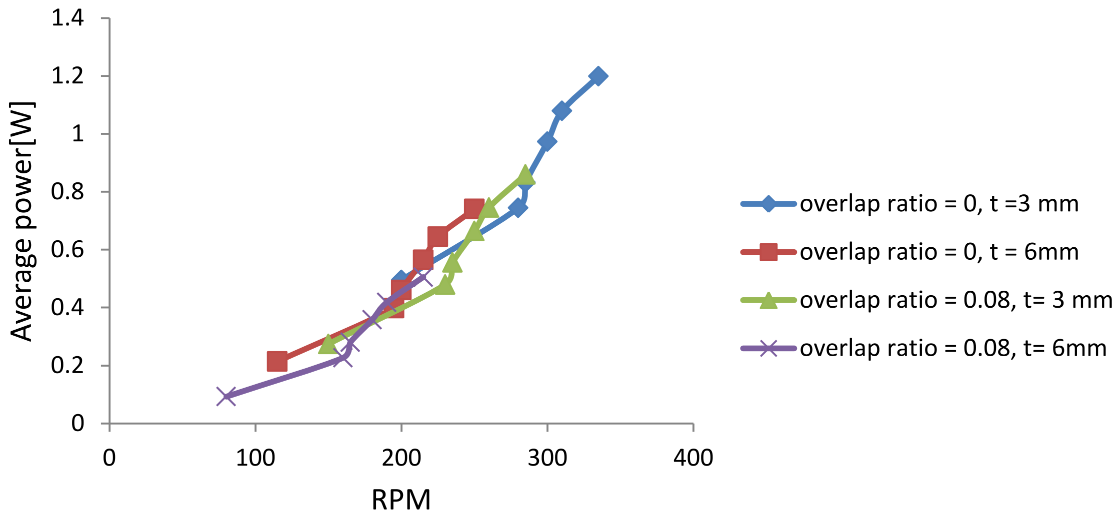

Figure 4.18: Average power change vs RPM at various overlap ratio and blade thickness with aspect ratio of 2.2

Table 4.4: Average power with respect to rotational speed (RPM) for L =30 mm

Aspect ratio 0.94, overlap ratio = 0.0, t = 3 mm						
RPM	145	225	230	245	255	280
Average Power [W]	0.120882	0.228469	0.293523	0.392042	0.468696	0.541861
Aspect ratio 0.94, overlap ratio = 0.0, t = 6 mm						
RPM	100	175	170	195	205	230
Average Power [W]	0.052549	0.123766	0.164561	0.251938	0.313618	0.374219
Aspect ratio 0.94, overlap ratio = 0.08, t = 3 mm						
RPM	95	175	180	195	205	230
Average Power [W]	0.051873	0.140361	0.194865	0.267964	0.324633	0.398573
Aspect ratio 0.94, overlap ratio = 0.08, t = 6 mm						
RPM	45	125	130	145	155	180
Average Power [W]	0.010703	0.061735	0.100673	0.154569	0.197686	0.256454
Aspect ratio 1.6, overlap ratio = 0.0, t = 3 mm						
RPM	180	260	265	280	290	315
Average Power [W]	0.279497	0.450972	0.528748	0.649393	0.741563	0.836107
Aspect ratio 1.6, overlap ratio = 0.0, t = 6 mm						
RPM	115	195	200	215	225	250
Average Power [W]	0.119499	0.23807	0.296328	0.388209	0.459783	0.535168
Aspect ratio 1.6, overlap ratio = 0.08, t = 3 mm						
RPM	130	210	215	230	240	265
Average Power [W]	0.111048	0.233151	0.299015	0.386941	0.454022	0.540893
Aspect ratio 1.6, overlap ratio = 0.08, t = 6 mm						
RPM	65	145	150	165	175	200
Average Power [W]	0.022138	0.086508	0.13157	0.192838	0.241172	0.305494
Aspect ratio 2.2, overlap ratio = 0.0, t = 3 mm						
RPM	200	280	285	300	310	335
Average Power [W]	0.49546	0.744534	0.832148	0.973141	1.079314	1.198916
Aspect ratio 2.2, overlap ratio = 0.0, t = 6 mm						
RPM	115	195	200	215	225	250
Average Power [W]	0.214008	0.398324	0.460691	0.5649	0.644691	0.740623
Aspect ratio 2.2, overlap ratio = 0.08, t = 3 mm						
RPM	150	230	235	250	260	285
Average Power [W]	0.479814	0.556168	0.664565	0.745593	0.859849	0.935478
Aspect ratio 2.2, overlap ratio = 0.08, t = 6 mm						
RPM	80	160	165	180	190	215
Average Power [W]	0.092992	0.226948	0.280326	0.358296	0.417988	0.505097

4.6 Effect of wind speed and overlap ratio for L =50 mm

The effect of wind speed and overlap ratio on the performace of the rotors with L =50 mm for various blade thickness (t = 3 mm and 6 mm) is discussed in this section.

a) Blade thickness (t) of 3 mm

Figures 4.19, 4.20 and 4.21 show the obtained static torque and power obtained for the optimal configuration as a function of rotor angle. It may be observed that the static torque and power values rise with the increase of wind speed and Blade height. Furthermore, it can be noticed that gap of new design of the rotors leads to drop off the static torque and power as shown from these figures. In comparison overlap ratio of 0.0 with overlap ratio of 0.08, the torque is apparently different each other as well as mechanical power, respectively. Hence, it is shown that the force acts on the rotor with overlap ratio 0.0 is greater than force acts on the rotor with overlap ratio 0.08 i.e. the force is decreasing inversely proportional with increasing the overlap ratio (or gap). As shown in these figures it is noticed that the force acting on the rotor (drag force) is increasing proportionally with increasing the blade height of the blade (increasing the aspect ratio).

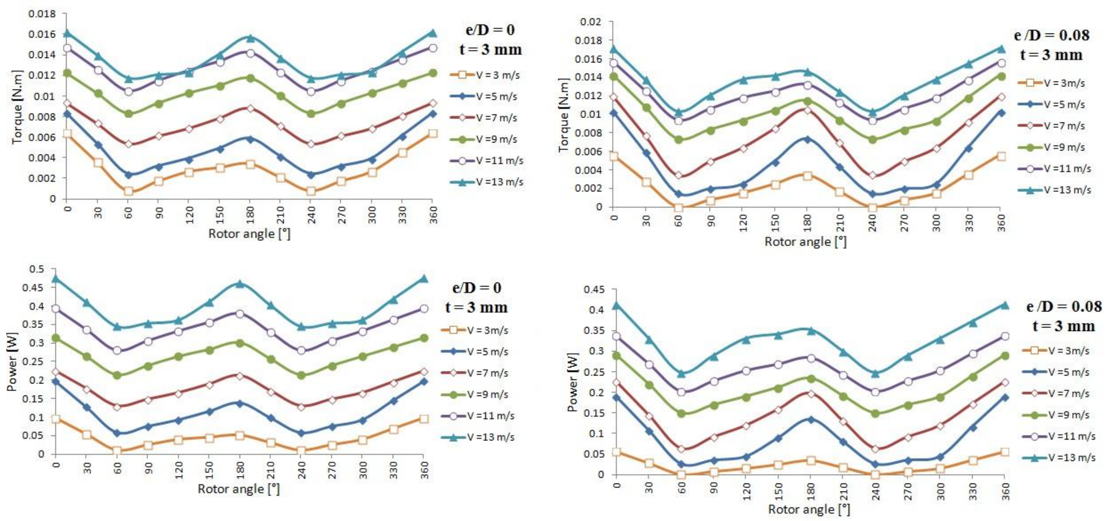

Figure 4.19: The torque change -rotor angle at various wind speed with aspect ratio of 0.94 and t =3 mm for L =50 mm

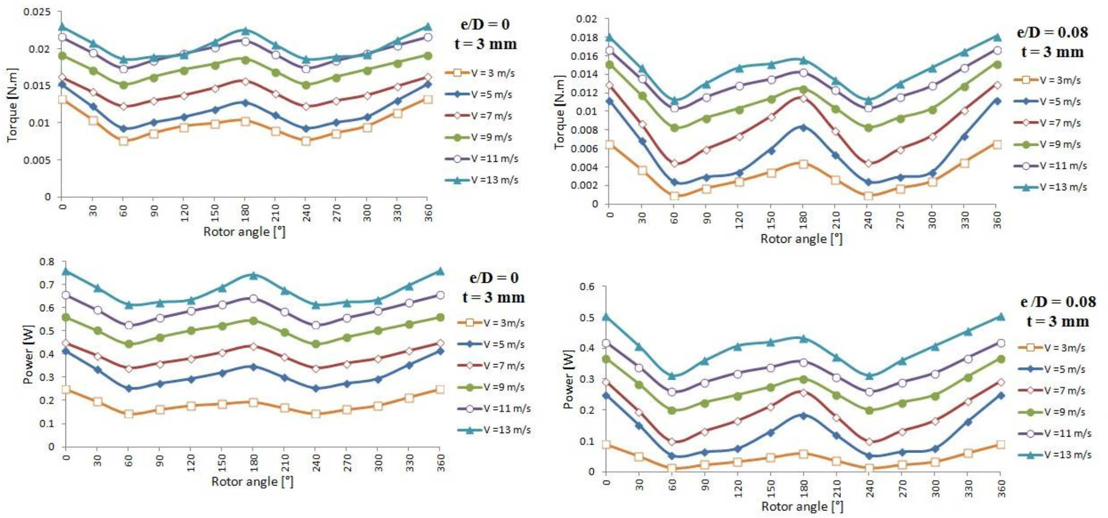

Figure 4.20: The torque change -rotor angle at various wind speed with aspect ratio of 1.6 and t =3 mm for L =50 mm

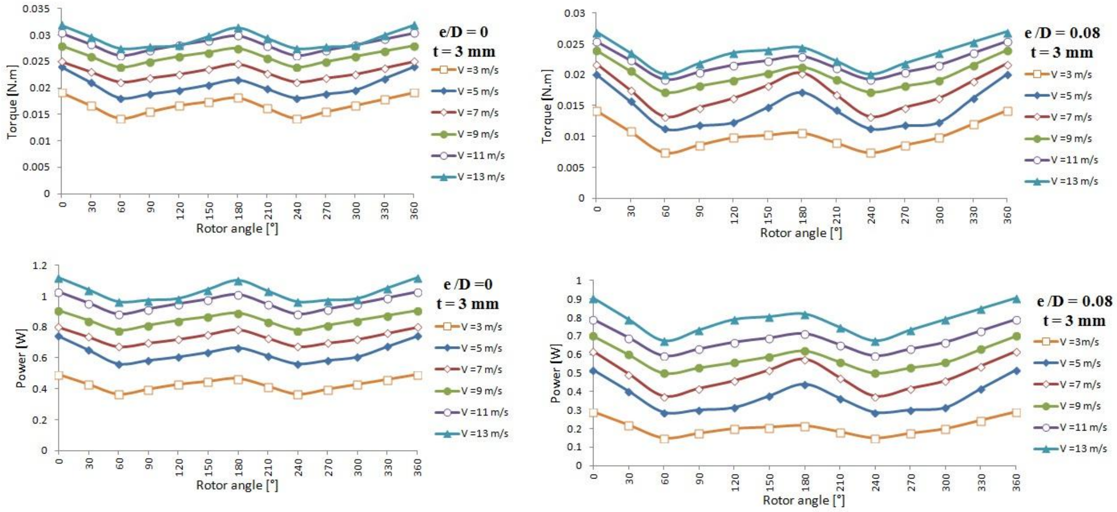

Figure 4.21: The torque change -rotor angle at various wind speed with aspect ratio of 2.2 and t =3 mm for L =50 mm

b) Blade thickness (t) of 6 mm

Similarly, it observed that the static torque and power of the rotors increase with increasing the blade height and wind speed as shown in Figures 422, 4.23 and 4.25. As well, these figures indicate the effect of overlap ratio on the static torque and power of the new configuration of Savonius wind rotors. It is seen that with the increase of overlap ratio, the static torque and power of the rotors decrease. Figures 422, 4.23 and 4.25 show the behavior of torque and mechanical power increasing with increasing variable blade height. As previously mentioned, increasing spring balance reader leads to decrease the difference between mass loaded and spring balance reader which is effect the acting force on the rotor i.e. the blade thickness of the rotor generally is inversely proportional to torque and mechanical power of the rotors.

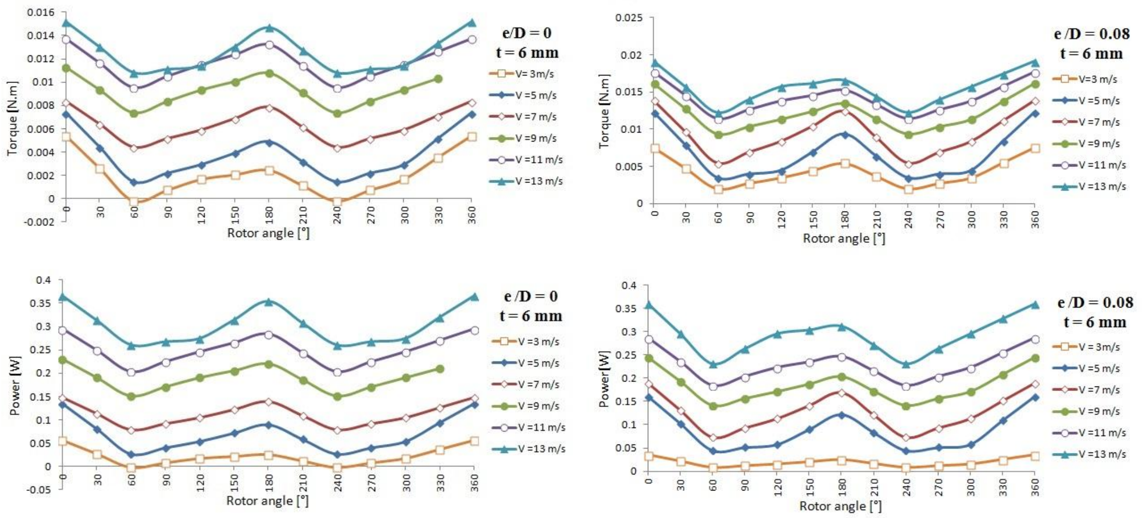

Figure 4.22: The torque change -rotor angle at various wind speed with aspect ratio of 0.94 and t =6 mm for L =50 mm

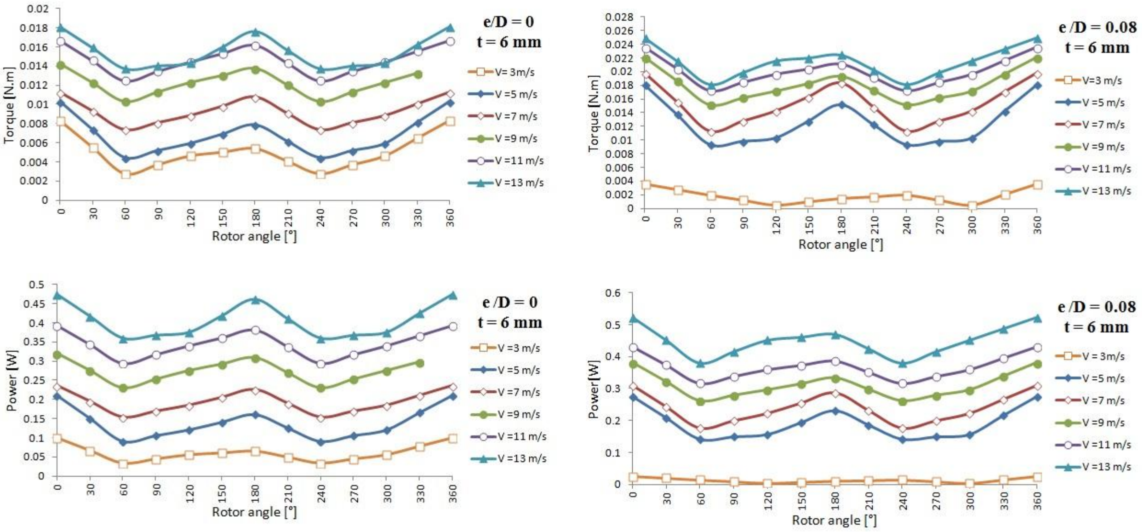

Figure 4.23: The torque change -rotor angle at various wind speed with aspect ratio of 1.6 and t =6 mm for L =50 mm

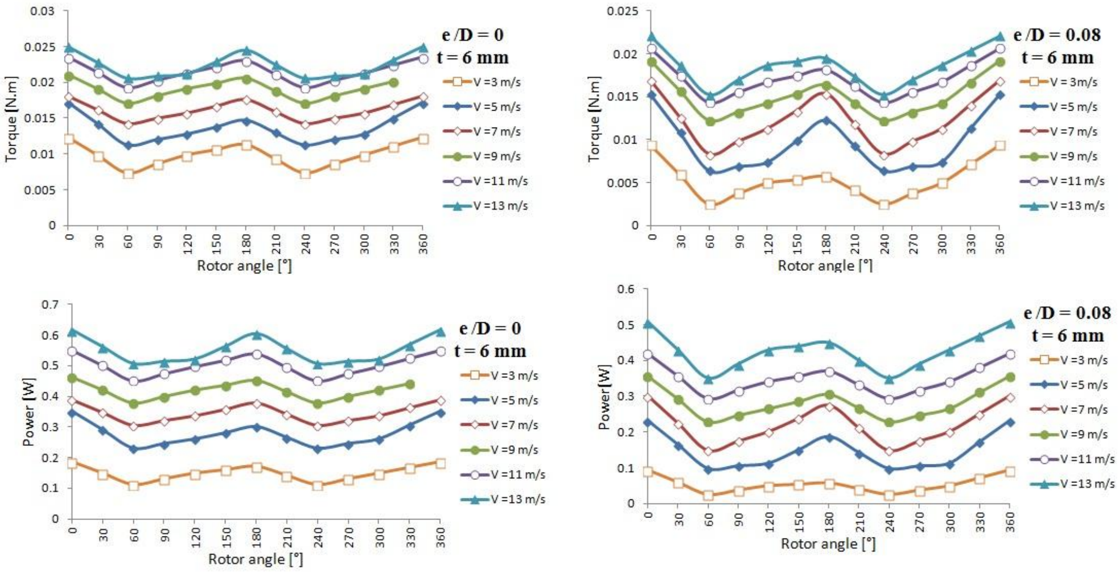

Figure 4.24: The torque change -rotor angle at various wind speed with aspect ratio of 2.2 and t =6 mm for L =50 mm

4.7 Relationship between Average Static Torques with Wind speed for L =50 mm

Figures 4.25, 4.26 and 4.27 demonstrate the average static torque for various tested blade profiles at wind speed of range from 3 m/s to13 m/s in steps of 2 m/s. when overlap ratio of 0.0, blade thickness, t = 3mm, and aspect ratio of 2.2, the average torque of the rotor is about 0.03N.m as shown in Table 4.5 and Figures 4.25, 4.26 and 4.27. Wind turbine model with overlap ratio 0.0 and blade thickness 3 mm has more drag force at any position when the wind rotor is in rotational position. Wind turbine rotor with high aspect ratio will deliver higher torque for the shaft of the turbine. Therefore, the highest aspect ratio and lowest overlap ratio leads to increase the torque of unconventional Savonius rotors as shown in Figures 4.25, 4.26 and 4.27 and Table 4.5.

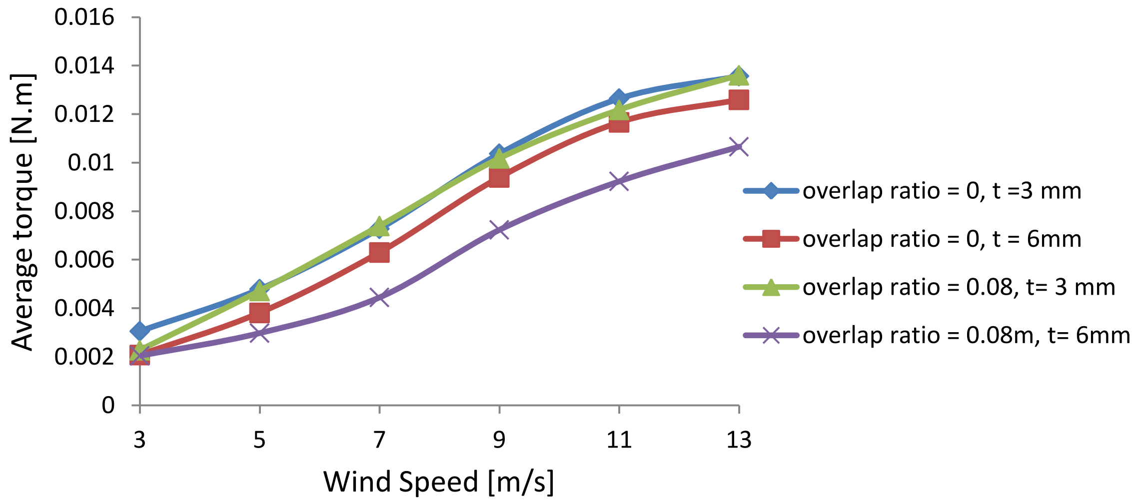

Figure 4.25: Average torque change vs wind speed at different overlap ratio and blade thickness with aspect ratio of 0.94 for L =50 mm

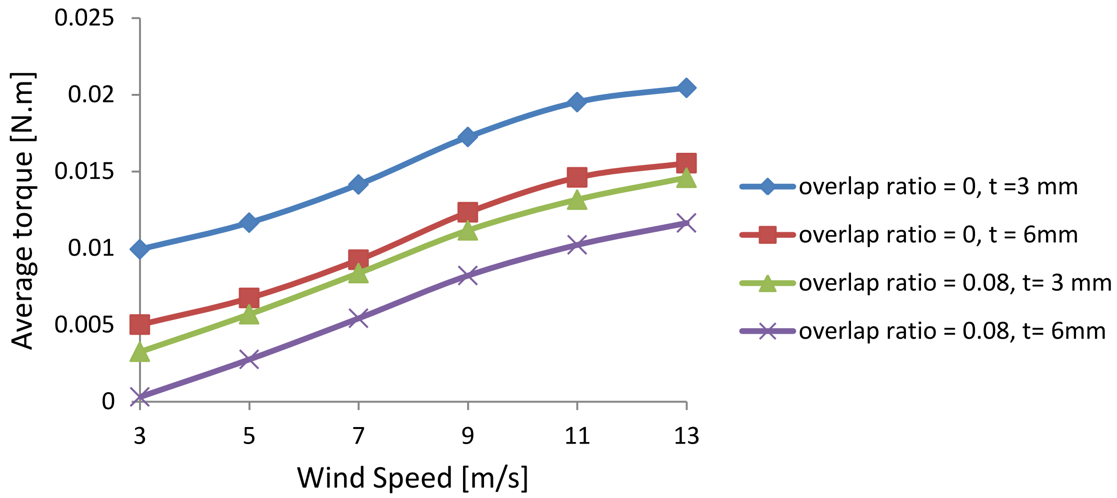

Figure 4.26: Average torque change vs wind speed at different overlap ratio and blade thickness with aspect ratio of 1.6 for L =50 mm

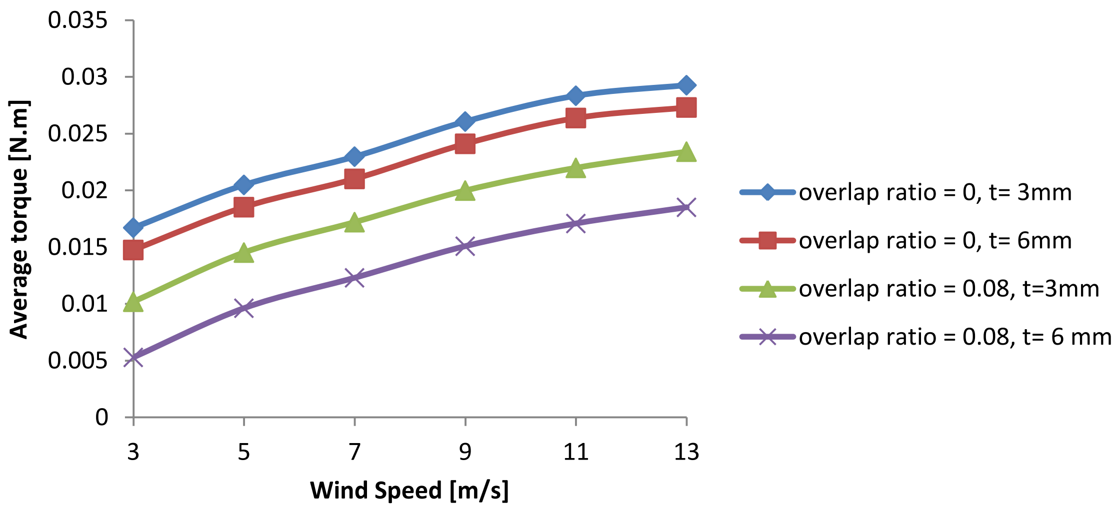

Figure 4.26: Average torque change vs wind speed at different overlap ratio and blade thickness with aspect ratio of 2.2 for L =50 mm

Table 4.5: Average static torque with respect to wind speed for L =50 mm

Aspect ratio = 0.94, overlap ratio = 0, t = 3 mm						
Wind speed [m/s]	3	5	7	9	11	13
Average torque[N.m]	0.003056	0.004792	0.007282	0.010376	0.012647	0.013576
Aspect ratio = 0.94, overlap ratio = 0, t = 6 mm						
Wind speed [m/s]	3	5	7	9	11	13
Average torque[N.m]	0.002075	0.003811	0.006301	0.009395	0.011666	0.012595
Aspect ratio = 0.94, overlap ratio = 0.08, t = 3 mm						
Wind speed [m/s]	3	5	7	9	11	13
Average torque[N.m]	0.002271	0.004716	0.007395	0.01018	0.012179	0.013606
Aspect ratio = 0.94, overlap ratio = 0.08, t = 6 mm						
Wind speed [m/s]	3	5	7	9	11	13
Average torque[N.m]	0.002045	0.002981	0.004452	0.007237	0.009236	0.010663
Aspect ratio = 1.6, overlap ratio = 0, t = 3 mm						
Wind speed [m/s]	3	5	7	9	11	13
Average torque[N.m]	0.009923	0.011659	0.014149	0.017243	0.019514	0.020443
Aspect ratio = 1.6, overlap ratio = 0, t = 6 mm						
Wind speed [m/s]	3	5	7	9	11	13
Average torque[N.m]	0.005018	0.006754	0.009244	0.012338	0.014609	0.015538
Aspect ratio = 1.6, overlap ratio = 0.08, t = 3 mm						
Wind speed [m/s]	3	5	7	9	11	13
Average torque[N.m]	0.003252	0.005697	0.008376	0.011161	0.01316	0.014587
Aspect ratio = 1.6, overlap ratio = 0.08, t = 6 mm						
Wind speed [m/s]	3	5	7	9	11	13
Average torque[N.m]	0.000309	0.002754	0.005433	0.008218	0.010217	0.011644
Aspect ratio = 2.2, overlap ratio = 0, t = 3 mm						
Wind speed [m/s]	3	5	7	9	11	13
Average torque[N.m]	0.016715	0.020488	0.022978	0.026072	0.028343	0.029272
Aspect ratio = 2.2, overlap ratio = 0, t = 6 mm						
Wind speed [m/s]	3	5	7	9	11	13
Average torque[N.m]	0.014753	0.018526	0.021016	0.02411	0.026381	0.02731
Aspect ratio = 2.2, overlap ratio = 0.08, t = 3 mm						
Wind speed [m/s]	3	5	7	9	11	13
Average torque[N.m]	0.010195	0.014526	0.017205	0.01999	0.021989	0.023416
Aspect ratio = 2.2, overlap ratio = 0.08, t = 6 mm						
Wind speed [m/s]	3	5	7	9	11	13
Average torque[N.m]	0.00529	0.009621	0.0123	0.015085	0.017084	0.018511

4.8 Relationship between Average Static Torques with RPM for L =50 mm

Table 4.6 shows the details of average static torque for L = 50 mm with different blade geometries and wind speed. It has been observed that the average torque for aspect ratio of 2.2, and blade thickness, t = 3 mm, is about 0.03 N.m, which is much higher than the other rotors as shown in Figures 4.27, 4.28 and 4.29. It can be concluded that the acting force on the rotor without gap (overlap ratio is equal to 0.0) and with highest aspect ratio is higher than other rotors. As a result, RPM is increased proportionally with increasing the acting force on the rotor

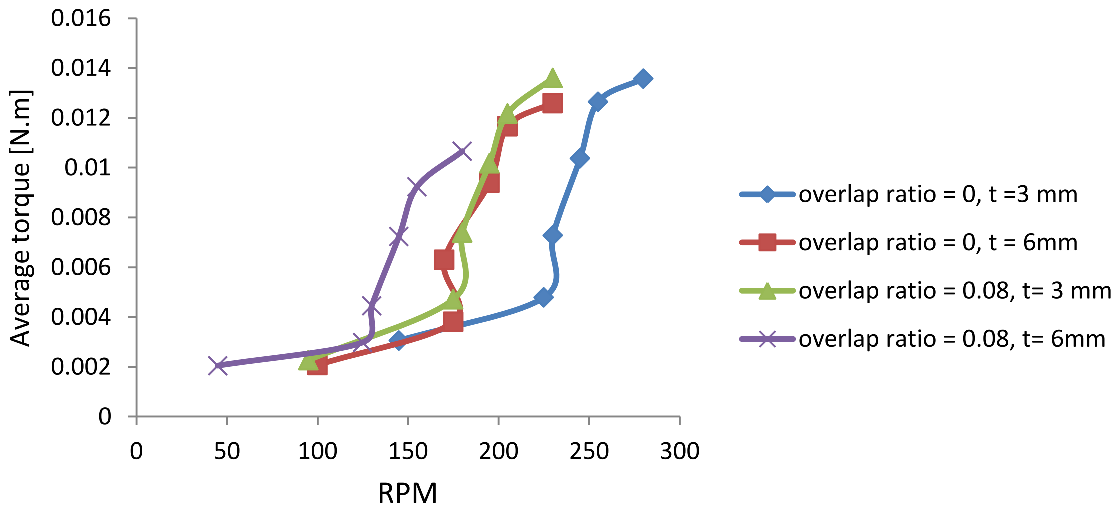

Figure 4.27: Average torque change vs RPM at different overlap ratio and blade thickness with aspect ratio of 0.94 for L = 50 mm

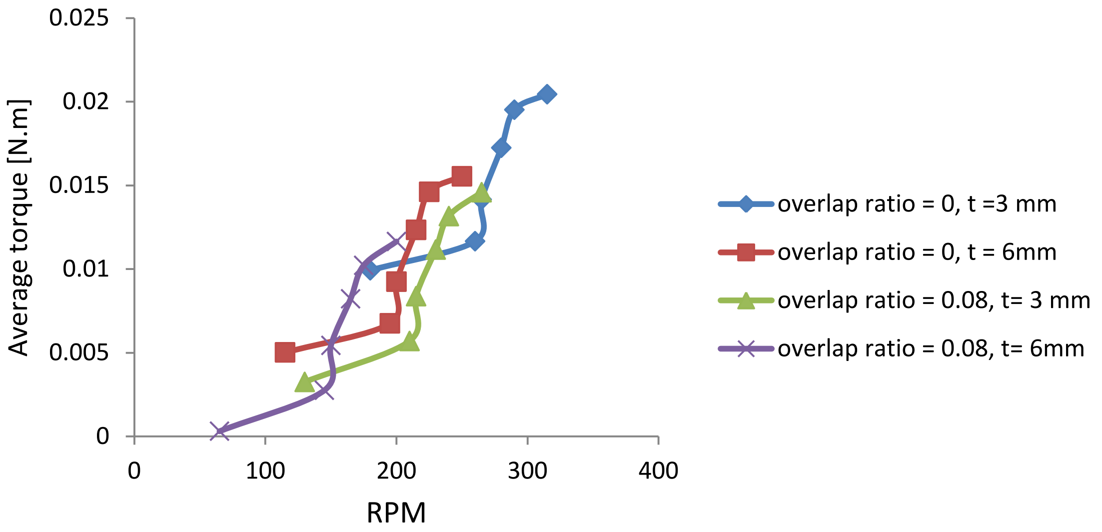

Figure 4.28: Average torque change vs RPM at different overlap ratio and blade thickness with aspect ratio of 1.6 for L = 50 mm

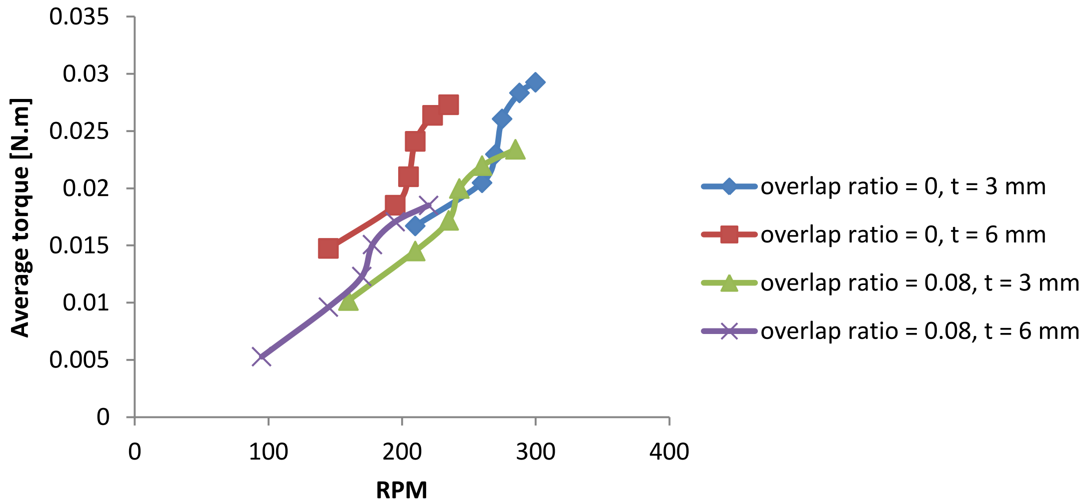

Figure 4.29: Average torque change vs RPM at different overlap ratio and blade thickness with aspect ratio of 2.2 for L = 50 mm

Table 4.6: Average static torque with respect to RPM for L =50 mm

Aspect ratio = 0.94, overlap ratio = 0, t = 3 mm						
RPM	145	225	230	245	255	280
Average torque[N.m]	0.003056	0.004792	0.007282	0.010376	0.012647	0.013576
Aspect ratio = 0.94, overlap ratio = 0, t = 6 mm						
RPM	100	175	170	195	205	230
Average torque[N.m]	0.002075	0.003811	0.006301	0.009395	0.011666	0.012595
Aspect ratio = 0.94, overlap ratio = 0.08, t = 3 mm						
RPM	95	175	180	195	205	230
Average torque[N.m]	0.002271	0.004716	0.007395	0.01018	0.012179	0.013606
Aspect ratio = 0.94, overlap ratio = 0.08, t = 6 mm						
RPM	45	125	130	145	155	180
Average torque[N.m]	0.002045	0.002981	0.004452	0.007237	0.009236	0.010663
Aspect ratio = 1.6, overlap ratio = 0, t = 3 mm						
RPM	180	260	265	280	290	315
Average torque[N.m]	0.009923	0.011659	0.014149	0.017243	0.019514	0.020443
Aspect ratio = 1.6, overlap ratio = 0, t = 6 mm						
RPM	115	195	200	215	225	250
Average torque[N.m]	0.005018	0.006754	0.009244	0.012338	0.014609	0.015538
Aspect ratio = 1.6, overlap ratio = 0.08, t = 3 mm						
RPM	130	210	215	230	240	265
Average torque[N.m]	0.003252	0.005697	0.008376	0.011161	0.01316	0.014587
Aspect ratio = 1.6, overlap ratio = 0.08, t = 6 mm						
RPM	65	145	150	165	175	200
Average torque[N.m]	0.000309	0.002754	0.005433	0.008218	0.010217	0.011644
Aspect ratio = 2.2, overlap ratio = 0, t = 3 mm						
RPM	210	260	270	275	288	300
Average torque[N.m]	0.016715	0.020488	0.022978	0.026072	0.028343	0.029272
Aspect ratio = 2.2, overlap ratio = 0, t = 6 mm						
RPM	145	195	205	210	223	235
Average torque[N.m]	0.014753	0.018526	0.021016	0.02411	0.026381	0.02731
Aspect ratio = 2.2, overlap ratio = 0.08, t = 3 mm						
RPM	160	210	235	243	260	285
Average torque[N.m]	0.010195	0.014526	0.017205	0.01999	0.021989	0.023416
Aspect ratio = 2.2, overlap ratio = 0.08, t = 6 mm						
RPM	95	145	170	178	195	220
Average torque[N.m]	0.00529	0.009621	0.0123	0.015085	0.017084	0.018511

4.9 Relationship between Average Powers with Wind Speed for L =50 mm

The effect of blade geometries and wind speed on the average power of the rotors are shown in Figures 4.30, 4.31 and 4.32 and it is tabulated in Table 4.7. In comparison, the highest average power value is about 1W which obtained from aspect ratio, overlap ratio and blade thickness of 2.2, 0.0 and 3 mm, respectively.

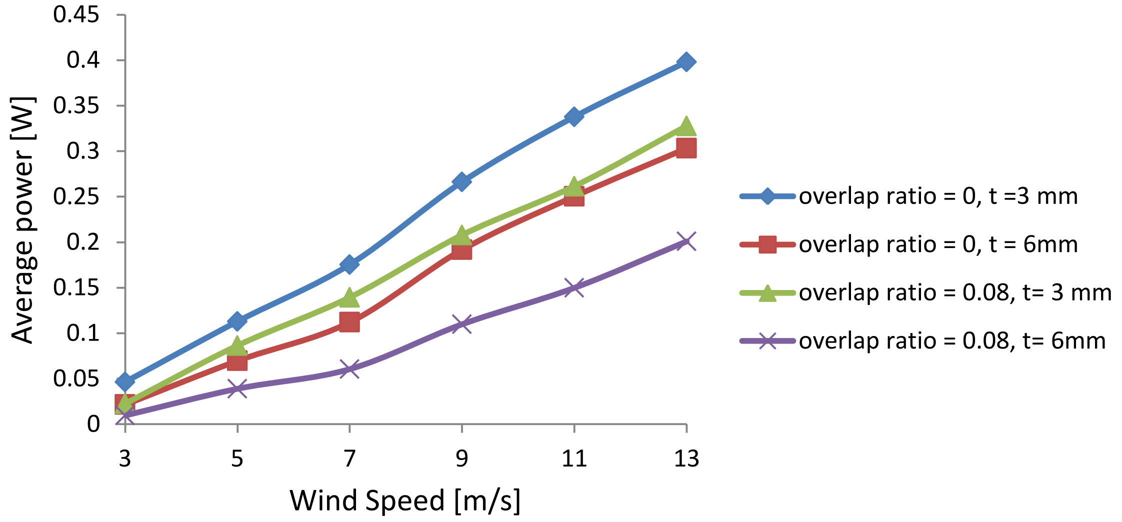

Figure 4.30: Average power change vs wind speed at different overlap ratio and blade thickness with aspect ratio of 0.94 for L = 50 mm

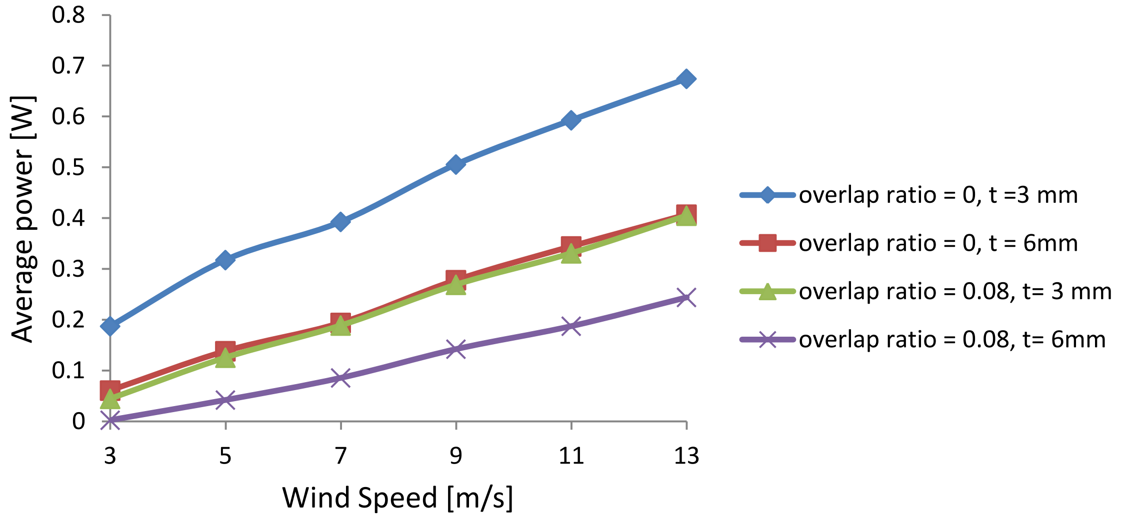

Figure 4.31: Average power change vs wind speed at different overlap ratio and blade thickness with aspect ratio of 1.6 for L = 50 mm

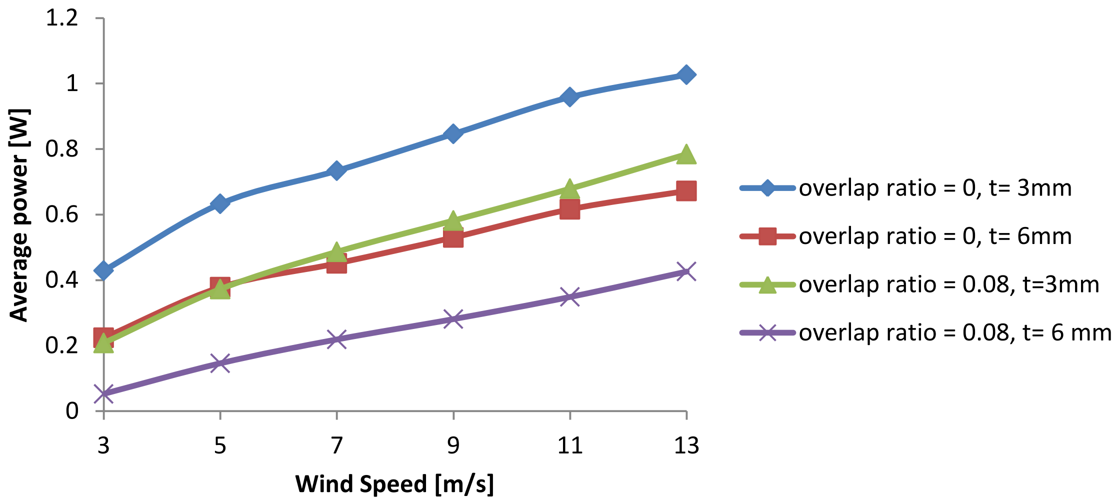

Figure 4.32: Average power change vs wind speed at different overlap ratio and blade thickness with aspect ratio of 2.2 for L = 50 mm

Table 4.7: Average power with respect to wind speed for L =50 mm

Aspect ratio = 0.94, overlap ratio = 0, t = 3 mm						
Wind speed [m/s]	3	5	7	9	11	13
Average Power [W]	0.046405	0.112901	0.175387	0.266201	0.337719	0.398044
Aspect ratio = 0.94, overlap ratio = 0, t = 6 mm						
Wind speed [m/s]	3	5	7	9	11	13
Average Power [W]	0.021731	0.069835	0.11217	0.191843	0.250441	0.303337
Aspect ratio = 0.94, overlap ratio = 0.08, t = 3 mm						
Wind speed [m/s]	3	5	7	9	11	13
Average Power [W]	0.022596	0.086429	0.139393	0.207868	0.261456	0.327691
Aspect ratio = 0.94, overlap ratio = 0.08, t = 6 mm						
Wind speed [m/s]	3	5	7	9	11	13
Average Power [W]	0.009637	0.039017	0.060609	0.109882	0.149918	0.200982
Aspect ratio = 1.6, overlap ratio = 0, t = 3 mm						
Wind speed [m/s]	3	5	7	9	11	13
Average Power [W]	0.187042	0.317427	0.392635	0.505575	0.592609	0.674312
Aspect ratio = 1.6, overlap ratio = 0, t = 6 mm						
Wind speed [m/s]	3	5	7	9	11	13
Average Power [W]	0.060431	0.137911	0.193601	0.277778	0.344215	0.40676
Aspect ratio = 1.6, overlap ratio = 0.08, t = 3 mm						
Wind speed [m/s]	3	5	7	9	11	13
Average Power [W]	0.044275	0.125287	0.188583	0.268805	0.330749	0.40478
Aspect ratio = 1.6, overlap ratio = 0.08, t = 6 mm						
Wind speed [m/s]	3	5	7	9	11	13
Average Power [W]	0.002106	0.041822	0.085342	0.141989	0.18724	0.243858
Aspect ratio = 2.2, overlap ratio = 0, t = 3 mm						
Wind speed [m/s]	3	5	7	9	11	13
Average Power [W]	0.428826	0.632897	0.733886	0.846352	0.958671	1.026848
Aspect ratio = 2.2, overlap ratio = 0, t = 6 mm						
Wind speed [m/s]	3	5	7	9	11	13
Average Power [W]	0.224004	0.378292	0.45115	0.53019	0.616053	0.672044
Aspect ratio = 2.2, overlap ratio = 0.08, t = 3 mm						
Wind speed [m/s]	3	5	7	9	11	13
Average Power [W]	0.372682	0.486452	0.581927	0.679287	0.784645	0.815374
Aspect ratio = 2.2, overlap ratio = 0.08, t = 6 mm						
Wind speed [m/s]	3	5	7	9	11	13
Average Power [W]	0.052624	0.14609	0.218967	0.281173	0.348861	0.426444

4.10 Relationship between Average Powers with RPM for L =50 mm

Figures 4.33-4.35 and Table 4.8 present the average power of new design of Savonius wind turbine rotors as function wind speed. It observed that as wind speed increases the average power of the rotor increases. Additionally, it can noticed that the increase in blade thickness and overlap ratio lead to decrease the average power of the rotors.

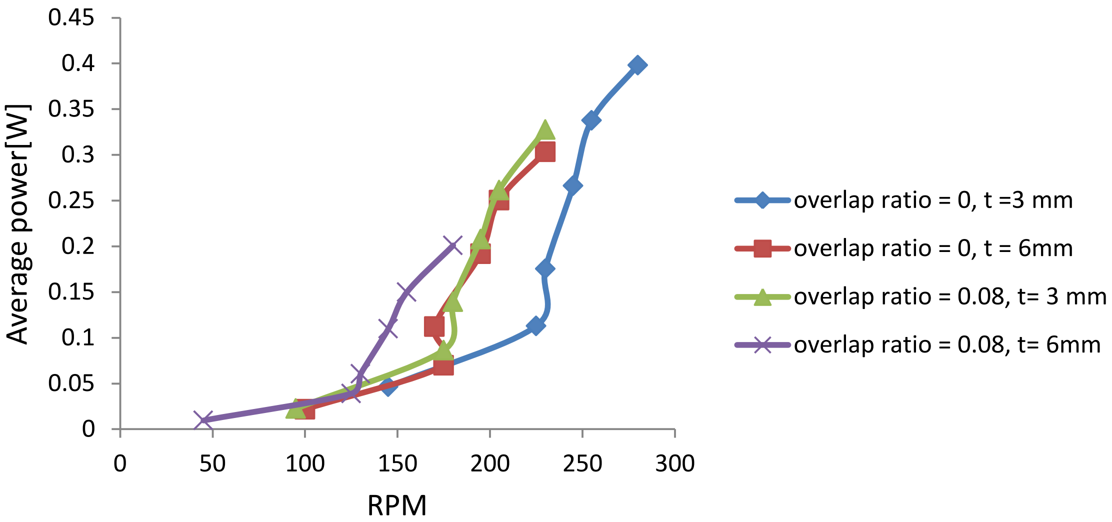

Figure 4.33: Average power change vs RPM at different overlap ratio and blade thickness with aspect ratio of 0.94 for L = 50 mm

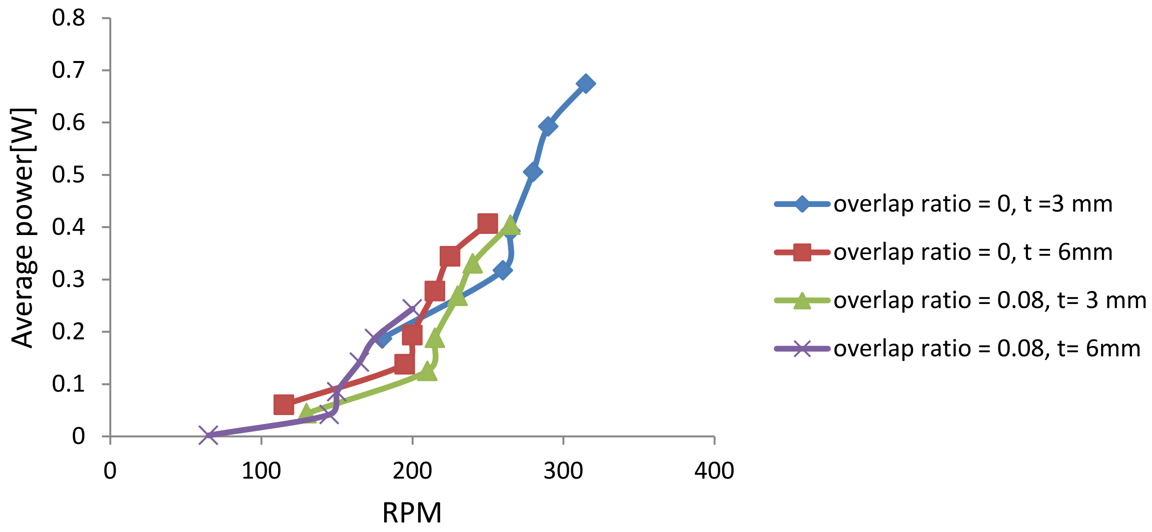

Figure 4.34: Average power change vs RPM at different overlap ratio and blade thickness with aspect ratio of 1.6 for L = 50 mm

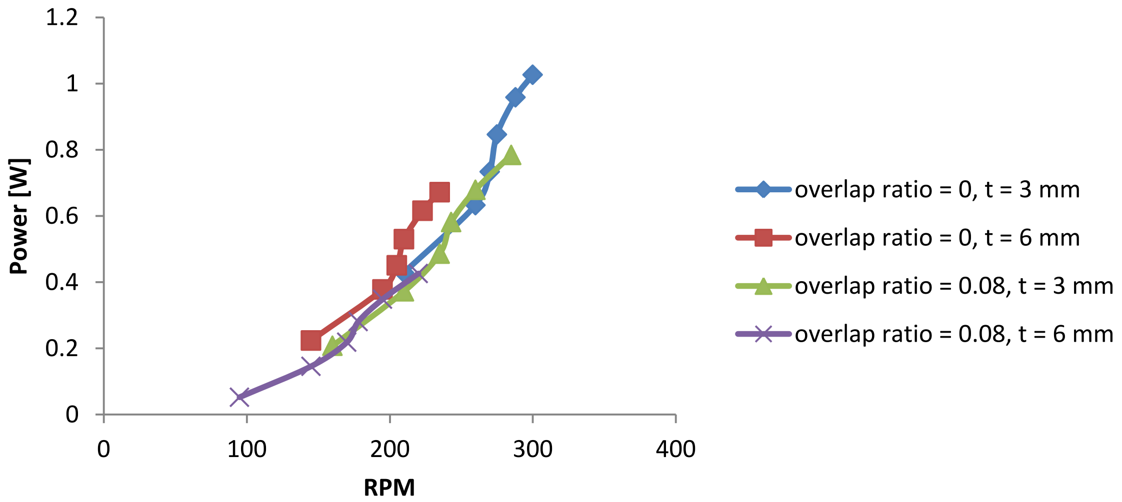

Figure 4.35: Average power change vs RPM at different overlap ratio and blade thickness with aspect ratio of 2.2 for L = 50 mm

Table 4.8: Average power with respect to RPM for L =50 mm

Aspect ratio = 0.94, overlap ratio = 0, t = 3 mm						
RPM	145	225	230	245	255	280
Average Power [W]	0.046405	0.112901	0.175387	0.266201	0.337719	0.398044
Aspect ratio = 0.94, overlap ratio = 0, t = 6 mm						
RPM	100	175	170	195	205	230
Average Power [W]	0.021731	0.069835	0.11217	0.191843	0.250441	0.303337
Aspect ratio = 0.94, overlap ratio = 0.08, t = 3 mm						
RPM	95	175	180	195	205	230
Average Power [W]	0.022596	0.086429	0.139393	0.207868	0.261456	0.327691
Aspect ratio = 0.94, overlap ratio = 0.08, t = 6 mm						
RPM	45	125	130	145	155	180
Average Power [W]	0.009637	0.039017	0.060609	0.109882	0.149918	0.200982
Aspect ratio = 1.6, overlap ratio = 0, t = 3 mm						
RPM	180	260	265	280	290	315
Average Power [W]	0.187042	0.317427	0.392635	0.505575	0.592609	0.674312
Aspect ratio = 1.6, overlap ratio = 0, t = 6 mm						
RPM	115	195	200	215	225	250
Average Power [W]	0.060431	0.137911	0.193601	0.277778	0.344215	0.40676
Aspect ratio = 1.6, overlap ratio = 0.08, t = 3 mm						
RPM	130	210	215	230	240	265
Average Power [W]	0.044275	0.125287	0.188583	0.268805	0.330749	0.40478
Aspect ratio = 1.6, overlap ratio = 0.08, t = 6 mm						
RPM	65	145	150	165	175	200
Average Power [W]	0.002106	0.041822	0.085342	0.141989	0.18724	0.243858
Aspect ratio = 2.2, overlap ratio = 0, t = 3 mm						
RPM	210	260	270	275	288	300
Average Power [W]	0.428826	0.632897	0.733886	0.846352	0.958671	1.026848
Aspect ratio = 2.2, overlap ratio = 0, t = 6 mm						
RPM	145	195	205	210	223	235
Average Power [W]	0.224004	0.378292	0.45115	0.53019	0.616053	0.672044
Aspect ratio = 2.2, overlap ratio = 0.08, t = 3 mm						
RPM	160	210	235	243	260	285
Average Power [W]	0.372682	0.486452	0.581927	0.679287	0.784645	0.81574
Aspect ratio = 2.2, overlap ratio = 0.08, t = 6 mm						
RPM	95	145	170	178	195	220
Average Power [W]	0.052624	0.14609	0.218967	0.281173	0.348861	0.426444

4.11 Comparison between L =30mm and L = 50 mm

In this section, the effect of length, L = 50mm and L = 30 mm, on the average power and torque at various blade geometries is studied. It can be observed that average torque and power of the rotors increase with increasing the blade height and reducing the length as shown in Figures 4.36 to 4.47. The working of a Savonius rotor depends greatly on the drag forces acting on their blades which vary along with the rotor blade angles. Due to this variation, the average torque and power on the rotor also varies with the rotor blade angles. Therefore, the drag force of the rotor without a gap, highest aspect ratio and lowest blade thickness is higher than other rotors. Because the pressure acting on the rotor (without gap, highest aspect ratio and lowest blade thickness) is higher than the pressure acting on the other rotors. As a result, the more blade surfaces with higher pressure is found when aspect ratio, overlap ratio, and blade thickness are equal to 2.2, 0.0 and 3mm, respectively i.e. high drag force means high torque and power produced by the rotors.

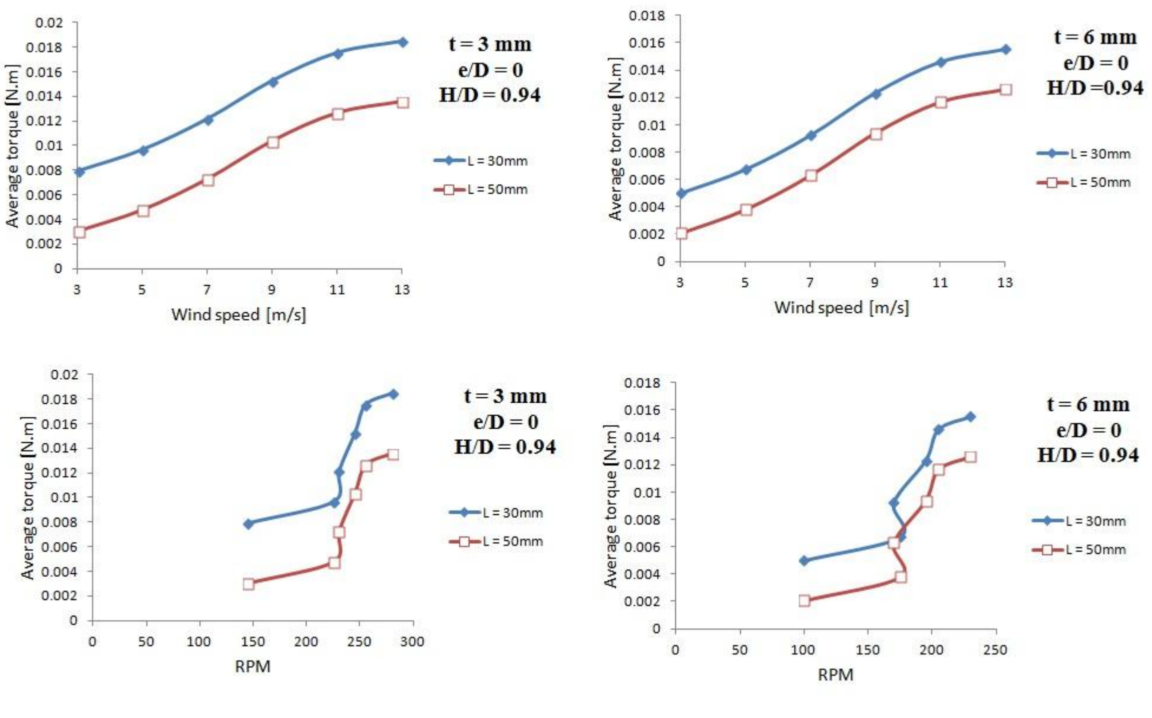

Figure 4.36: Comparison average torque between L = 30mm and 50mm for aspect ratio of 0.94 and overlap ratio of 0.0

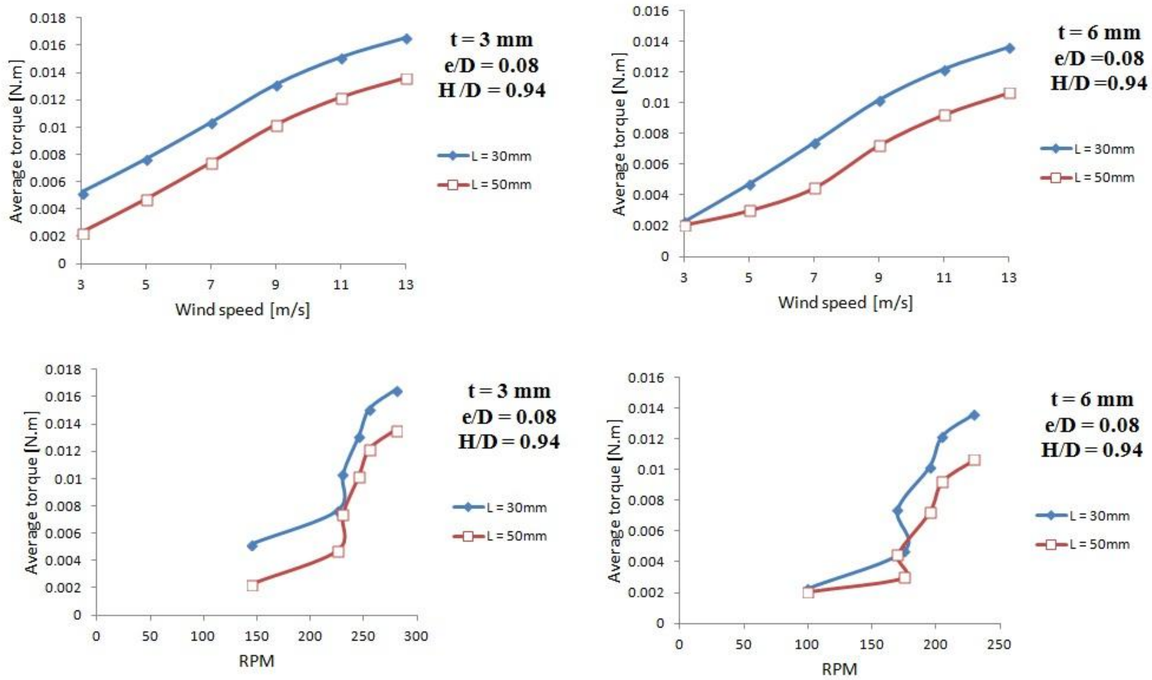

Figure 4.37: Comparison average torque between L = 30mm and 50mm for aspect ratio of 0.94 and overlap ratio of 0.08

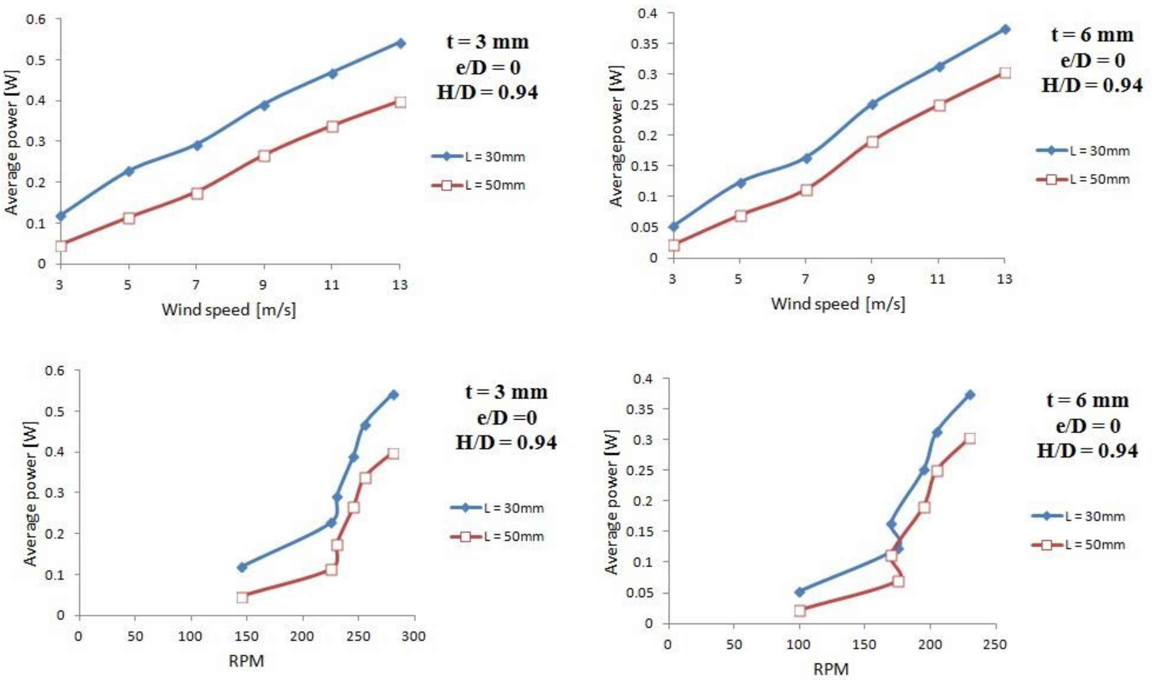

Figure 4.38: Comparison average power between L = 30mm and 50mm for aspect ratio of 0.94 and overlap ratio of 0.0

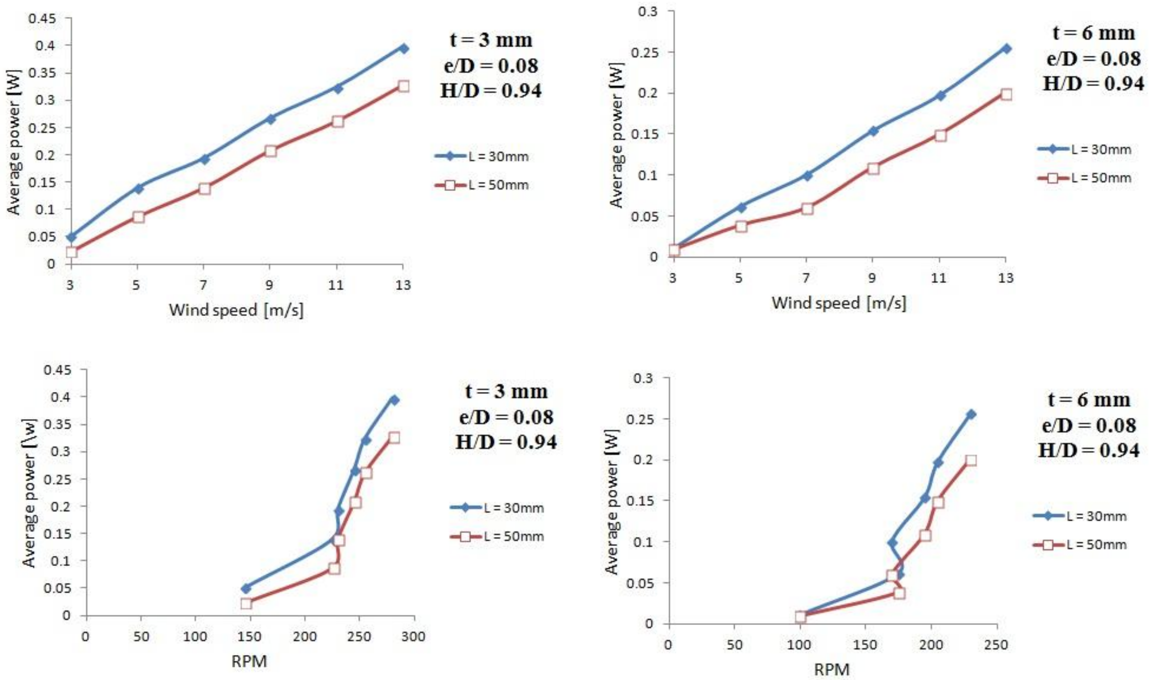

Figure 4.39: Comparison average power between L = 30mm and 50mm for aspect ratio of 0.94 and overlap ratio of 0.08

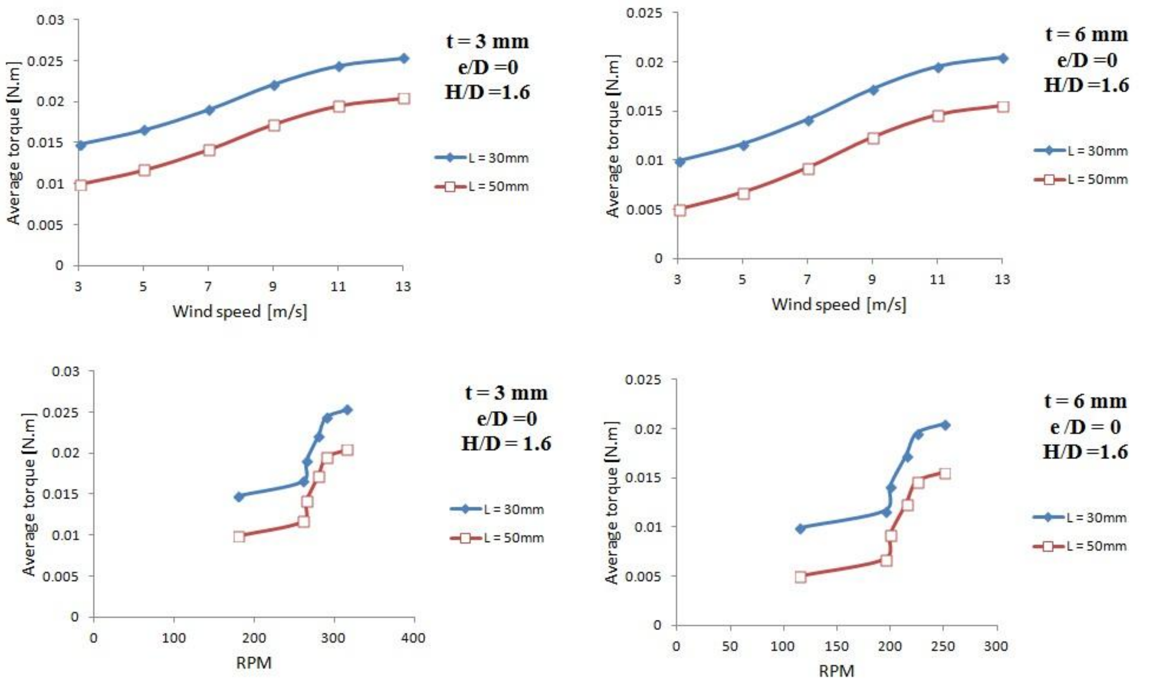

Figure 4.40: Comparison average torque between L = 30mm and 50mm for aspect ratio of 1.6 and overlap ratio of 0.0

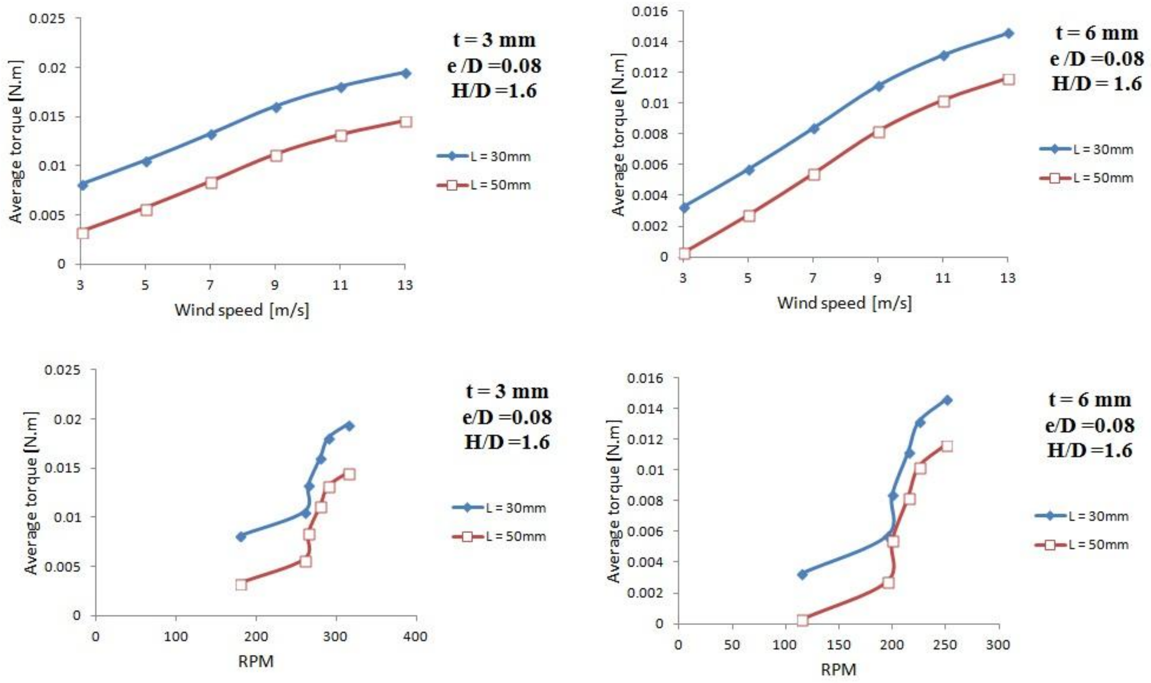

Figure 4.41: Comparison average torque between L = 30mm and 50mm for aspect ratio of 1.6 and overlap ratio of 0.08

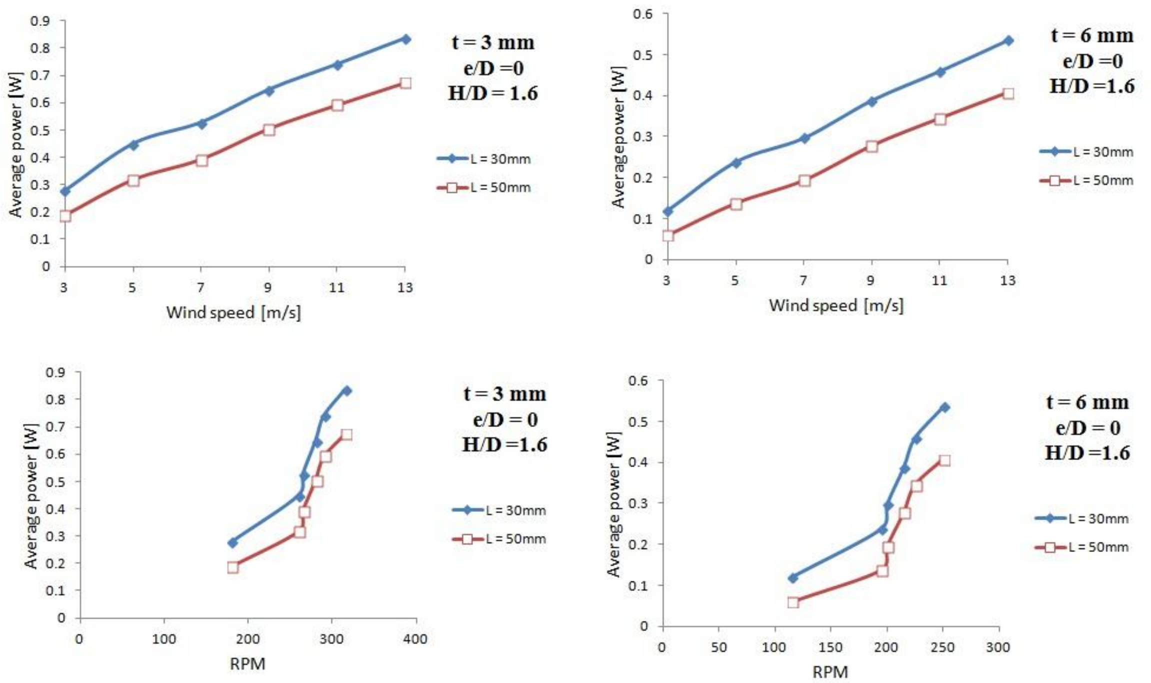

Figure 4.42: Comparison average power between L = 30mm and 50mm for aspect ratio of 1.6 and overlap ratio of 0.0

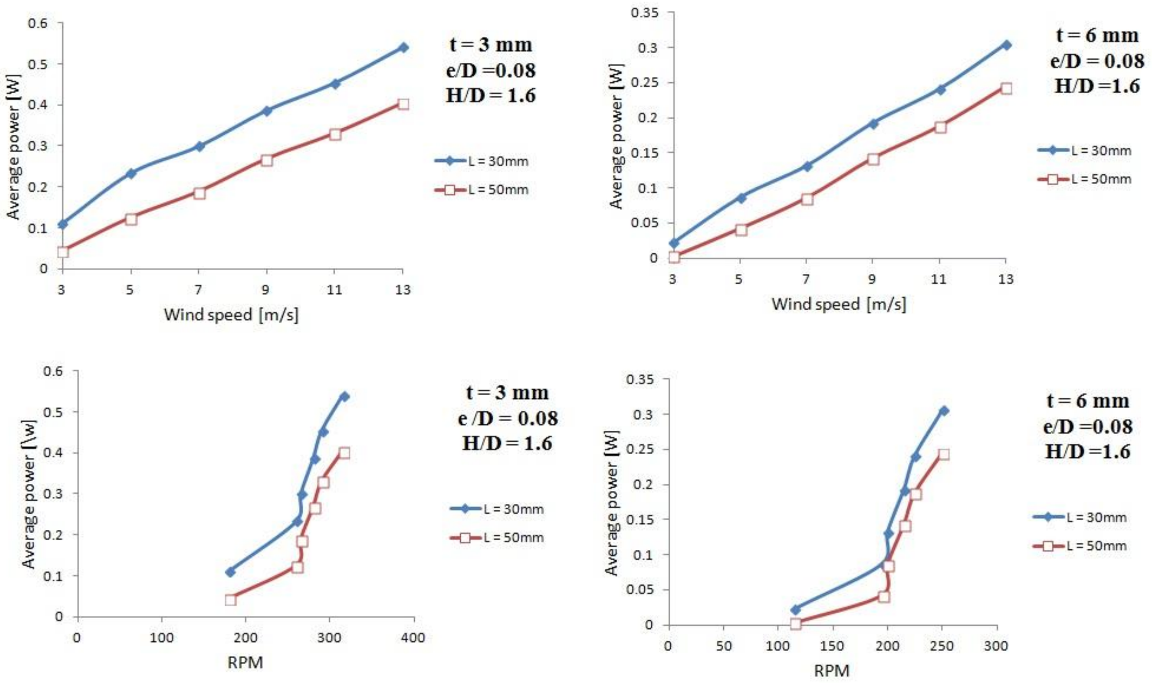

Figure 4.43: Comparison average power between L = 30mm and 50mm for aspect ratio of 1.6 and overlap ratio of 0.08

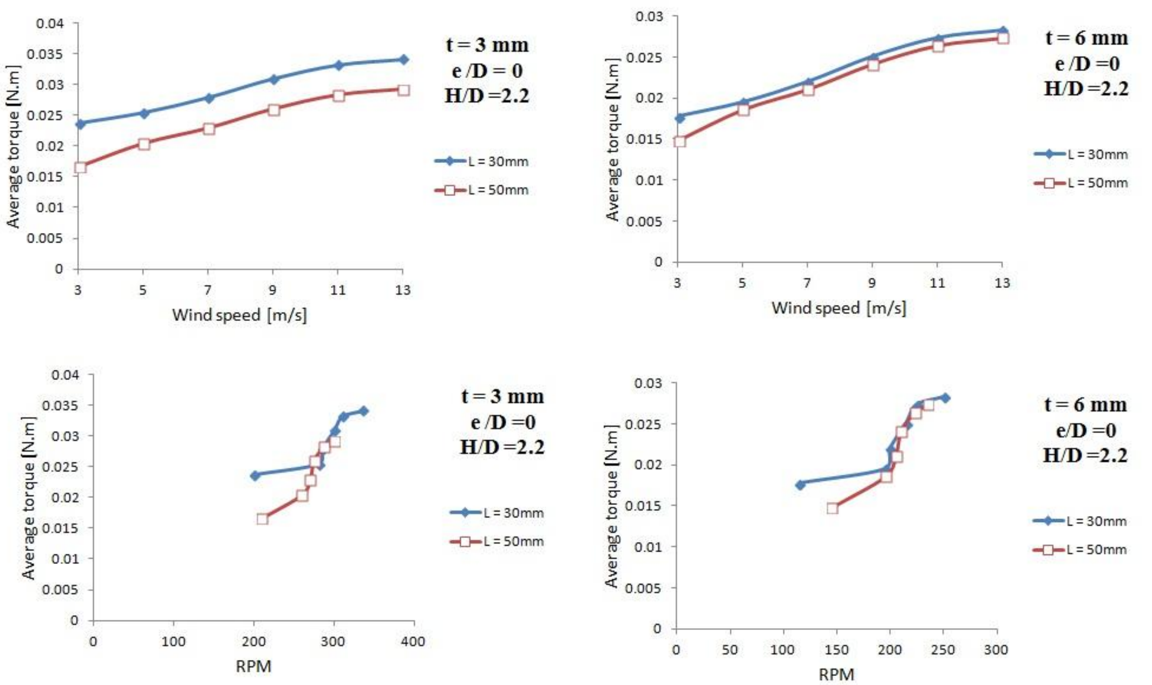

Figure 4.44: Comparison average torque between L = 30mm and 50mm for aspect ratio of 2.2 and overlap ratio of 0.0

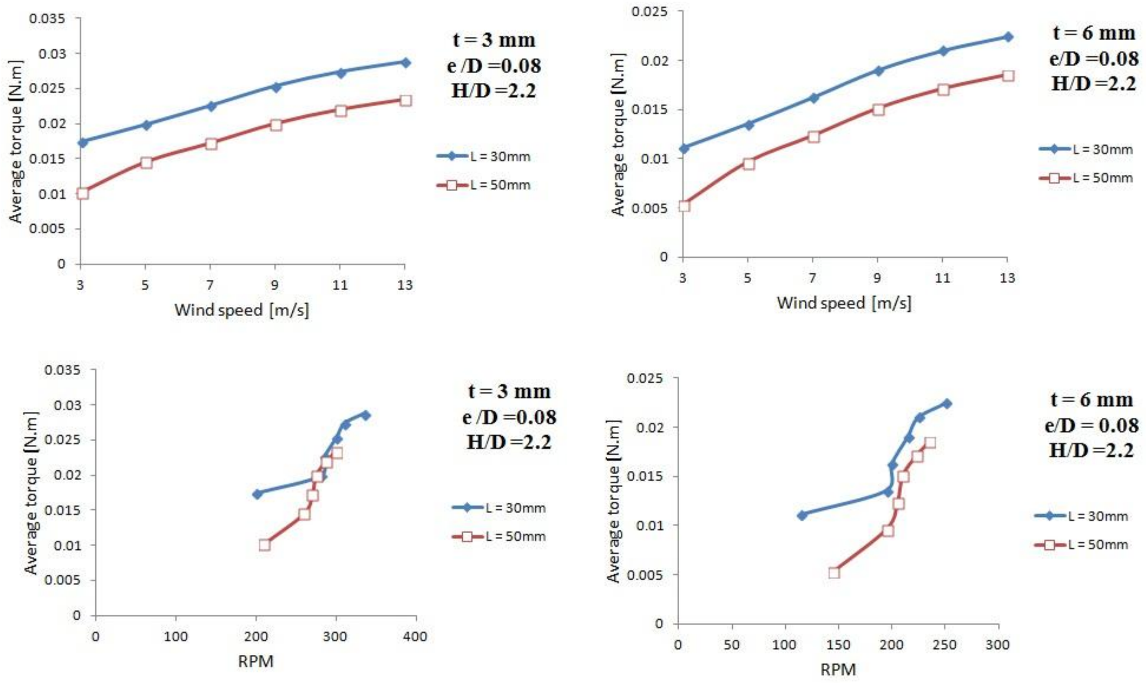

Figure 4.45: Comparison average torque between L = 30mm and 50mm for aspect ratio of 2.2 and overlap ratio of 0.08

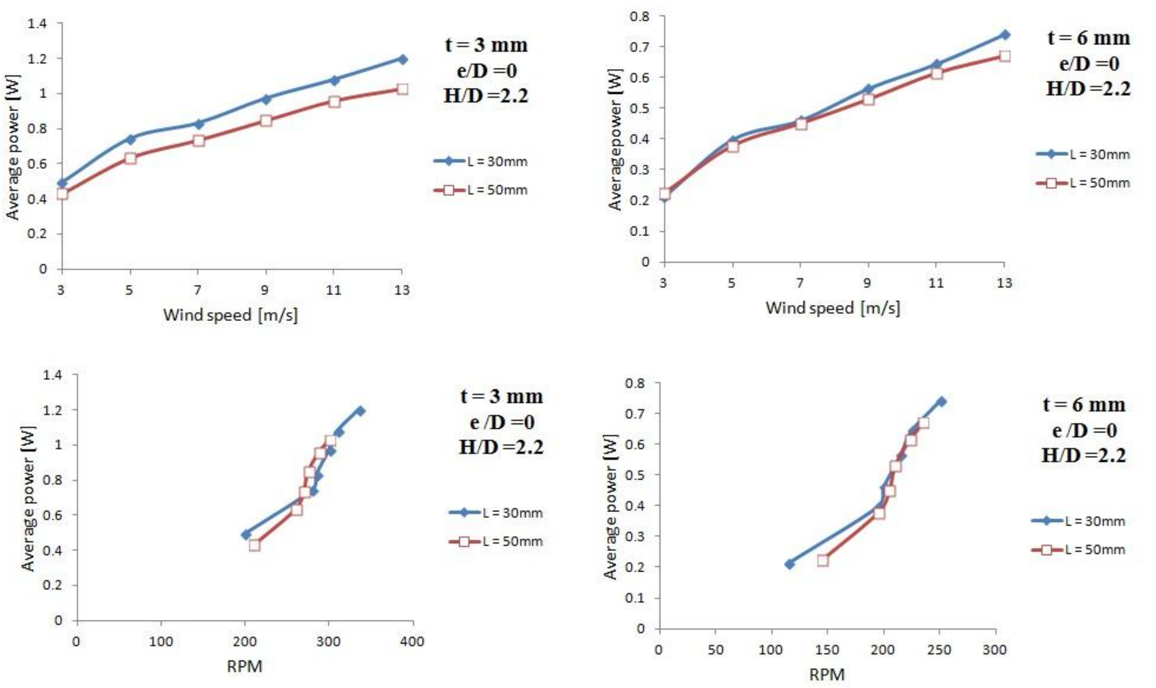

Figure 4.46: Comparison average power between L = 30mm and 50mm for aspect ratio of 2.2 and overlap ratio of 0.0

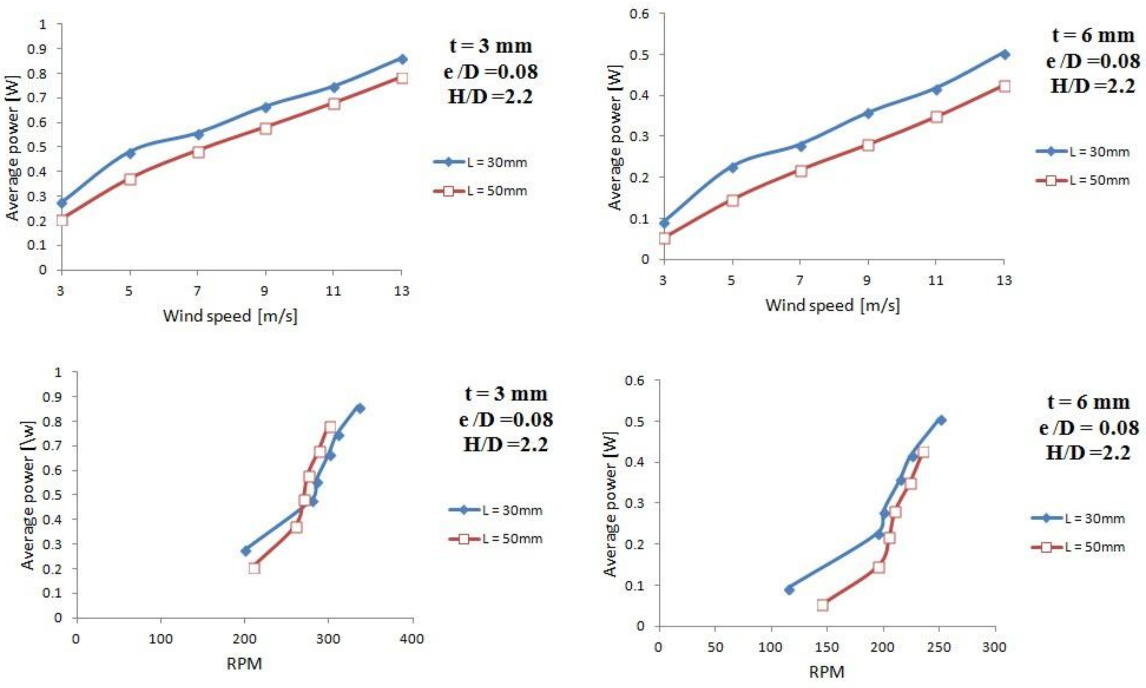

Figure 4.48: Comparison average power between L = 30mm and 50mm for aspect ratio of 2.2 and overlap ratio of 0.0

4.12 Comparison experimental results with Previous Study

In this section, it shows the difference the torque value, which calculated by recording spring balance reader and torque value, which obtained from Driss (2015) by using the same dimension of Savonius wind turbine, and wind speed as shown in Table 6.2. The blade of an unconventional Savonius wind turbine, which obtained from Driss (2015) was made from fiberglass with a diameter of 100 mm, blade height of 200 mm and blade thickness of t = 6 mm. While the blade of the unconventional Savonius wind turbine of this work was made from PVC material. It is noticed that the percentage error between both values of RPM and torque is about 10 percent and 13.6, respectively.

CHAPTER 5
CONCLUSION AND FUTURE WORK

Based on this study, the objectives of this work have been accomplished. The major findings are reviewed below.

5.1 Conclusion

In this research, the improvement of the performance of new configuration of Savonius rotor at low wind speed has been studied experimentally. Therefore, the rotors have been designed and placed in front of open wind tunnel with velocity ranges of 0 m/s to 15 m/s. The results obtained from this experimental study are:

- The study showed that the static torque and mechanical power increase with increasing of aspect ratio and decreasing overlap ratio.
- It found that mechanical power of unconventional rotors increases by reducing the overlap ratio and increasing the aspect ratio.
- Blade geometries will influence the rotation of the rotor of Savonius wind turbine models. The rotor with aspect ratio of 2.2, overlap ratio of 0.0 and blade thickness of 3 mm blade produces higher mechanical power than other rotors.
- Increasing in blade thickness leads to decrease the static torque and mechanical power of the unconventional Savonius wind turbine.
- The results obtained that, the static torque and mechanical power at all the rotor angles for all unconventional Savonius rotors tested in this study are positive.
- It was also found that the largest bladed height and thickness (H = 700mm, t = 6 mm) turbine shook violently during testing. At high wind speed and large blade rotors, the turbine is shook violently and unstable which leads to reduce the performance of the rotor.

5.2 Future Works

In order to make some improvement in the performances of unconventional Savonius rotors, there are some recommended actions that could be done to further improve the results calculated from this study:

- The materials of Savonius wind turbine blade rotors should be improved by using some lighter materials and more durable so that it could be able to withstand any high pressures caused by the wind for some period of time.
- Further research will aim at developing and optimizing the Savonius wind turbine under static, dynamic and fatigue conditions. Also, the parameters of Savonius wind turbine rotor will be fully analyzed to enhance its effectiveness.

REFERENCES

Adaramola, M. (2014). *Wind turbine technology: Principles and design*. Waretown, NJ: Apple Academic Press, Inc.

Ajedegba, J. (2008). *Effect of Blade Configuration on Flow Distribution and Power Output of a Zephir Vertical Axis Wind Turbine* (Unpublished doctoral dissertation). University of Ontario Institute of Technology.

Ali, M. (2013). Experimental Comparison Study for Savonius Wind Turbine of Two & Three Blades At Low Wind Speed. *International Journal of Modern Engineering Research (IJMER), 3*(5), 2978-2986.

Altan, B. D., & Atılgan, M. (2008b). An experimental and numerical study on the improvement of the performance of Savonius wind rotor. *Energy Conversion and Management*, *49*(12), 3425-3432.

Altan, B. D., Atılgan, M., & Özdamar, A. (2008a). An experimental study on improvement of a Savonius rotor performance with curtaining. *Experimental Thermal and Fluid Science*, *32*(8), 1673-1678.

Bhadra, S. N., Banerjee, S., & Kastha, D. (2005). *Wind electrical systems*. New Delhi [Inde: Oxford University Press.

Bhatti, T., & Kothari, D. (2003). Aspects of Technological Development of Wind Turbines. *J. Energy Eng*, *129*(3), 81–95.

Chiras, D. D., Sagrillo, M., & Woofenden, I. (2009). *Power from the wind*. Gabriola Island, BC: New Society Publishers.

Daut, I., Razliana, A., Irwan, Y., & Farhana, Z. (2012). A Study on the Wind as Renewable Energy in Perlis, Northern Malaysia. *Energy Procedia*, *18*, 1428-1433.

Dinçer, I., & Zamfirescu, C. (2012). *Sustainable Energy Systems and Applications*. Boston, MA: Springer Science+Business Media, LLC.

Dixon, K. (2008). *The Near Wake Structure of a Vertical Axis Wind Turbine* (Master's thesis, Delft University of Technology). Retrieved from Delft University of Technology.

Driss, Z. (2015). Evaluation of the Savonius Wind Rotor Performance for Different External Overlap Ratios. *International Journal of Fluid Mechanics & Thermal Sciences*, *1*(1), 14.

Driss, Z., Mlayeh, O., Driss, S., Driss, D., Maaloul, M., & Abid, M. S. (2015). Study of the bucket design effect on the turbulent flow around unconventional Savonius wind rotors. *Energy*, *89*, 708-729. doi:10.1016/j.energy.2015.06.023

Eriksson, S., Bernhoff, H., & Leijon, M. (2008). Evaluation of different turbine concepts for wind power. *Renewable and Sustainable Energy Reviews*, *12*(5), 1419-1434.

Eriksson, S., Bernhoff, H., & Leijon, M. (2008). Evaluation of different turbine concepts for wind power. *Renewable and Sustainable Energy Reviews*, *12*(5), 1419-1434.

Fujisawa, N. (1992). On the torque mechanism of Savonius rotors. *Journal of Wind Engineering and Industrial Aerodynamics*, *40*(3), 277-292.

Gasch, R., & Twele, J. (2012). *Wind Power Plants: Fundamentals, Design, Construction and Operation*. Berlin, Heidelberg: Springer Berlin Heidelberg.

Ghosh, T. K., & Prelas, M. A. (2011). *Energy resources and systems: Volume 2*. Dordrecht: Springer.

Gipe, P. (1995). *Wind energy comes of age*. New York: Wiley.

Gipe, P. (2003). *Wind power: Renewable energy for home, farm, and business* (2nd ed.). White River Junction, VT: Chelsea Green Pub. Co.

Gosselin, R., Dumas, G., & Boudreau, M. (2016). Parametric study of H-Darrieus vertical-axis turbines using CFD simulations. *Journal of Renewable and Sustainable Energy*, *8*(5), 053301.

Harrison, R., Hau, E., & Snel, H. (2000). *Large wind turbines: Design and economics*. Chichester [etc.: Wiley & Sons.

Hemami, A. (2012). *Wind turbine technology*. Clifton Park, NY: Delmar, Cengage Learning.

Howell, R., Qin, N., Edwards, J., & Durrani, N. (2010). Wind tunnel and numerical study of a small vertical axis wind turbine. *Renewable Energy*, *35*(2), 412-422.

Kamoji, M., Kedare, S., & Prabhu, S. (2009). Performance tests on helical Savonius rotors. *Renewable Energy*, *34*(3), 521-529. doi:10.1016/j.renene.2008.06.002

Ledec, G., Rapp, K. W., & Aiello, R. (2011). *Greening the wind: Environmental and social considerations for wind power development*. Washington, DC: World Bank.

MacKay, D. J. (2009). *Sustainable energy--without the hot air*. Cambridge, England: UIT.

Mahmoud, N., El-Haroun, A., Wahba, E., & Nasef, M. (2012). An experimental study on improvement of Savonius rotor performance. *Alexandria Engineering Journal*, *51*(1), 19-25. doi:10.1016/j.aej.2012.07.003

Mani, A., & Mooley, D. A. (1983). *Wind energy data for India*. New Delhi: Allied.

Mathew, S. (2006). *Wind energy: Fundamentals, resource analysis and economics ; with 31 tables*. Berlin [u.a.: Springer.

Medaglia, M. (2010). *Vertical Axis Wind Turbines: History, Technology and Applications* (Master's thesis). Retrieved from http://www.diva-portal.org/smash/get/diva2:326493/fulltext01

Menet, J. (2004). A double-step Savonius rotor for local production of electricity: a design study. *Renewable Energy*, *29*(11), 1843-1862.

Npowers. (2007). Project Components. Retrieved November 13, 2016, from www.natwindpower.co.uk/gwyntymor/components.asp

Paul, A. (2010). *A Comparative Analysis of the Two-Bladed and the Three- Bladed Wind Turbine for Offshore Wind Farms* (Master's thesis, Technical University of Delft).

Rashid, M. (2007). *Power Electronics Handbook* (3rd ed.). USA: Elsevier.

Ricci, R., Romagnoli, R., Montelpare, S., & Vitali, D. (2016). Experimental study on a Savonius wind rotor for street lighting systems. *Applied Energy*, *161*, 143-152.

Ricci, R., Vitali, D., & Montelpare, S. (2014). An innovative wind–solar hybrid street light: development and early testing of a prototype. *International Journal of Low-Carbon Technologies*, *10*(4), 420-429.

Rivkin, D. A., Randall, M., & Silk, L. (2014). *Wind power generation and distribution*. Burlington, MA: Jones & Bartlett Learning.

Sheldahl, R., Feltz, L., & Blackwell, B. (1978). Wind tunnel performance data for two- and three-bucket Savonius rotors. *Journal of Energy*, *2*(3), 160-164.

Shepherd, W., & Zhang, L. (2010). *Electricity generation using wind power*. Singapore: World Scientific.

Shigetomi, A., Murai, Y., Tasaka, Y., & Takeda, Y. (2011). Interactive flow field around two Savonius turbines. *Renewable Energy*, *36*(2), 536-545.

Tong, W. (2010). *Wind power generation and wind turbine design*. Southampton: WIT Press.

Turner, W. C. (2005). *Energy management handbook: By Wayne C. Turner* (5th ed.). Lilburn, GA: Fairmont Press.

United States. (2000). *Renewable energy issues and trends*. Washington, DC: Energy Information Administration, Office of Coal, Nuclear, Electric and Alternate Fuels, U.S. Dept. of Energy.

Wagner, H., & Mathur, J. (2014). *Introduction to Wind Energy Systems: Basics, Technology and Operation*. Berlin: Springer Berlin.

Wood, D. (2011). *Small wind turbines: analysis, design, and application*: Springer